

# LIBRARY Michigan State University

This is to certify that the thesis entitled

Ultrathin, Multilayered Polyelectrolyte Films as Nanofiltration Membranes

presented by

Brian W. Stanton

has been accepted towards fulfillment of the requirements for the

M.S. degree in Chemistry

Major Professor's Signature

12/11/03

Date

MSU is an Affirmative Action/Equal Opportunity Institution

# PLACE IN RETURN BOX to remove this checkout from your record. TO AVOID FINES return on or before date due. MAY BE RECALLED with earlier due date if requested.

DATE DUE	DATE DUE	DATE DUE

6/01 c:/CIRC/DateDue.p65-p.15

# Ultrathin, Multilayered Polyelectrolyte Films as Nanofiltration Membranes

Ву

Brian W. Stanton

#### A THESIS

Submitted to
Michigan State University
in partial fulfillment of the requirements
for the degree of

MASTER OF SCIENCE

Department of Chemistry

2003

#### **ABSTRACT**

Ultrathin, Multilayer Polyelectrolyte Films as Nanofiltration Membranes

By

#### Brian W. Stanton

This thesis shows that alternating polyelectrolyte deposition on porous supports yields nanofiltration membranes that allow high water flux along with selective ion Membranes composed of 4.5 to 5 layer pairs of poly(styrene transport. sulfonate) (PSS)/poly(allylamine hydrochloride) (PAH) on porous alumina allow water fluxes of 1 to 2 m<sup>3</sup>m<sup>-2</sup>d<sup>-1</sup> at 4.8 bar while exhibiting MgSO<sub>4</sub> rejections of 96%. In general, divalent-ion rejection increases when the charge of the outer layer of the membrane matches that of the ion being rejected. Increasing the concentration of supporting electrolyte present during deposition of the terminating PSS layer results in a higher surface charge density, and hence higher Na<sub>2</sub>SO<sub>4</sub> rejections. The use of PSS/poly(diallyldimethylammonium chloride) bilayers as a gutter layer underneath the selective PSS/PAH skin allows for higher water fluxes on both alumina and polymeric supports. Preliminary research shows that the use of polyelectrolyte films for nanofiltration may allow for repair of fouled membranes. Removal of the surface layer (along with fouling material) from the membrane using high pH buffer, and adsorption of a new surface layer may regenerate the membranes.

Dedicated to my wife Angela and to my parents.

#### **ACKNOWLEDGMENTS**

I gratefully acknowledge financial support of this work by the US Department of Energy Office of Basic Energy Sciences and Pall Corporation. We also thank Keith Harris of DOW Chemical for fruitful discussions and the design of the nanofiltration apparatus. I would also like to thank Dan Sullivan and Matt Miller for taking FESEM pictures for this research.

# **TABLE OF CONTENTS**

List of Tables	vi
List of Figures	vii
List of Abbreviations	viii
Chapter 1. Introduction	1
Chapter 2. Nanofiltration of Salt Solutions Using Multi-layered	11
Polyelectrolyte Membranes on Alumina Supports	
Chapter 3. Development of Composite Polyelectrolyte NF	33
Membranes on Polymeric Supports	
Chapter 4. Fouling and Repair of NF Membranes (Future Work)	53

# LIST OF TABLES

Table 2.1.	Ion rejection and water flux for various polyelectrolyte nanofiltration membranes using a 1000 ppm salt concentration in the feed solution.	22
Table 2.2.	Ion rejection and water flux for various polyelectrolyte nanofiltration membranes using a 50 ppm salt concentration in the feed solution.	23
Table 2.3.	Percent rejection values for individual anions and water fluxes from NF experiments with mixed salt solutions.	28
Table 2.4.	Cl <sup>-</sup> /SO <sub>4</sub> <sup>2-</sup> selectivities from single-salt and mixed-salt NF experiments.	29
Table 3.1.	Ellipsometric thicknesses for PSS/PDADMAC films on aluminum or gold-coated substrates.	39
Table 3.2.	Cl <sup>-</sup> and SO <sub>4</sub> <sup>2-</sup> % rejections, water fluxes, and Cl <sup>-</sup> /SO <sub>4</sub> <sup>2-</sup> selectivities for NF with MPF membranes deposited on alumina using a PSS/PDADMAC gutter layer.	41
Table 3.3.	Water flux and % rejection values in NF of CaCl <sub>2</sub> and MgSO <sub>4</sub> solutions by MPFs containing a PSS/PDADMAC gutter layer on alumina.	44
Table 3.4.	Percent rejection of Cl <sup>-</sup> and SO <sub>4</sub> <sup>2-</sup> as well as water flux in NF with various membranes prepared by MPF deposition on PES 100 supports.	47
Table 4.1.	Ellipsometric thickness values for 5-bilayer PAH/PSS films before and after submersion in buffer solutions.	62
Table 4.2.	Absorbances for the 3 main peaks in the spectra in Figure 4.4.	65

# **LIST OF FIGURES**

Figure 1.1.	Schematic diagram of the alternating deposition process used to form a polyelectrolyte film on a porous alumina support.	2
Figure 1.2.	Cross-sectional view of a fouled membrane on a porous support.	7
Figure 2.1.	The chemical structures of the polyelectrolytes used in this study.	13
Figure 2.2.	Experimental setup for nanofiltration experiments.	16
Figure 2.3.	Schematic diagram of the nanofiltration membrane cell.	17
Figure 3.1.	Field emission scanning eletron microscopy (FESEM) image of the surface of a bare Pall Corporation 100 kD ultrafiltration membrane.	34
Figure 3.2.	Shows the chemical structure of PDADMAC.	37
Figure 3.3.	Cross-sectional FESEM image of [PSS/PDADMAC] <sub>3</sub> [PSS/PAH]PSS deposited on porous alumina.	41
Figure 3.4.	FESEM image of a [PSS/PDADMAC] <sub>7</sub> [PSS/PAH]PSS film (final PSS layer deposited from 2.5 M MnCl <sub>2</sub> ) deposited on PES100	48
Figure 4.1.	Plot of water flux vs. time for the NF of a 50 ppm Mg <sup>2+</sup> solution (added as MgSO <sub>4</sub> ) containing 20 mg/L of humic acid.	57
Figure 4.2.	Plot of the Mg <sup>2+</sup> concentration in the permeate vs. time when filtering a 50 ppm Mg <sup>2+</sup> (from MgSO₄) solution containing 20 mg/L humic acid.	58
Figure 4.3.	Plot of $SO_4^{2-}$ concentration in the permeate solution vs. time when filtering a 50 ppm $Mg^{2+}$ (from $MgSO_4$ ) solution containing 20 mg/L of humic acid.	59
Figure 4.4.	ERFTIR spectra of PAH/PSS films on a gold-coated silicon wafer.	64

#### LIST OF ABBREVIATIONS

Abbreviation Meaning of abbreviation

NF Nanofiltration

MPF Multilayer polyelectrolyte film

PSS Poly(styrene sulfonate)

PAH Poly(allylamine hydrochloride)

NOM Natural Organic Matter

PAA Poly(acrylic acid)

MPA 3-mercaptopropionic acid

FESEM Field emission scanning electron microscopy

PDADMAC Poly(diallyldimethylammonium chloride)

Abs Absorbance

AFM Atomic force microscopy

PES Poly(ethersulfone)

ERFTIR External reflectance Fourier transform infrared

spectroscopy

#### Chapter 1

#### INTRODUCTION

Nanofiltration (NF) is an important membrane-based separation process for applications such as water softening, wastewater reclamation, and dye-salt separations.<sup>1-6</sup> Fluxes and analyte rejections in NF are between those of ultrafiltration and reverse osmosis, and thus, NF affords rejection of large molecules or multivalent ions along with a relatively high water flux at low operating pressures (<14 bar).<sup>2,7</sup> This thesis investigates the use of alternating polyelectrolyte deposition as a method of creating NF membranes for potential industrial applications.

To achieve high water flux, the majority of NF membranes consist of a thin, selective skin deposited on a thick, permeable support, *e.g.*, an ultra or microfiltration membrane. The composition of the selective layer determines the separation characteristics of the membrane, while the support provides mechanical stability to the system. Typically, solute transport through NF membranes is a function of the charge and pore size in the skin layer.<sup>7-10</sup> Thus, in NF of ions, the membrane skin is usually highly charged and has an effective pore size between 1 and 5 nm.<sup>8-13</sup>

Adsorption of multilayered polyelectrolyte films (MPFs) on porous supports is a relatively new technique that provides a simple way to create charged, ultrathin membrane skins.<sup>14-19</sup> This technique is attractive because it affords

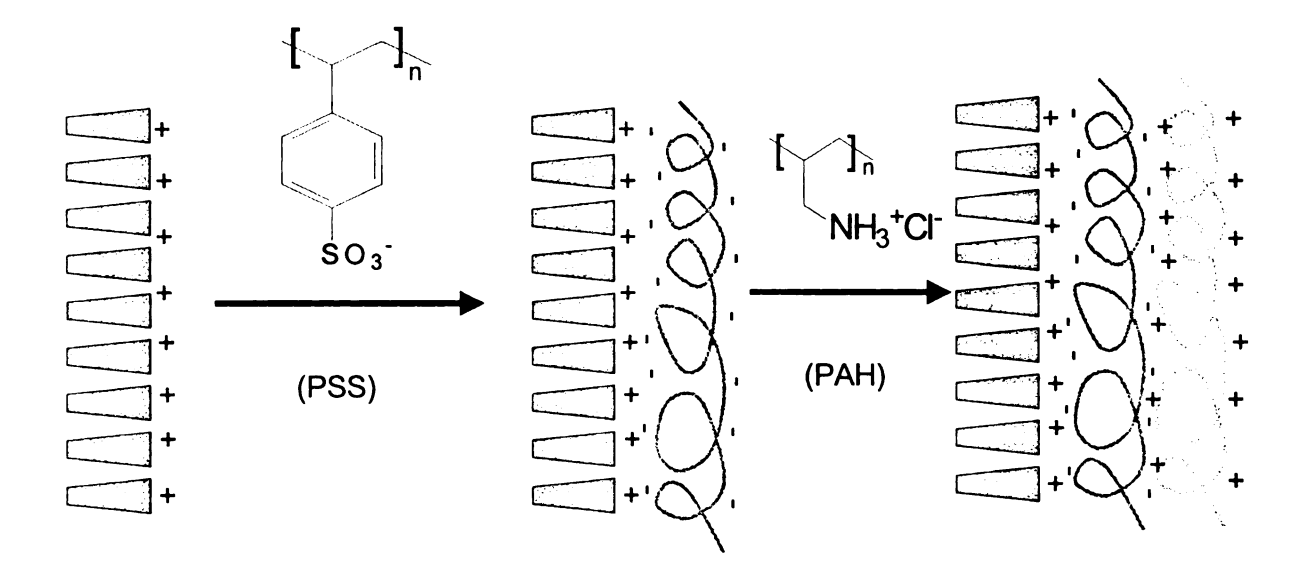


**Figure 1.1**: Schematic diagram of the alternating deposition process used to form a polyelectrolyte film on a porous alumina support. This process can be repeated as many times as needed to prepare multilayer films.

control over the thickness, charge density, and composition of the active skin layer.<sup>20</sup> Deposition of MPFs simply involves alternating immersions of a charged substrate into solutions containing oppositely charged polyelectrolytes (figure 1.1), and film thickness depends on the number of polyelectrolyte layers as well as the pH and supporting salt concentration in the polyelectrolyte solutions.<sup>21-27</sup> As virtually any polyelectrolyte can form MPFs,<sup>28-32</sup> alternating polyelectrolyte deposition is capable of forming a wide variety of membranes.

Several groups performed fundamental studies of transport through MPFs. 15,23,33-39 Möhwald and von Klitzing examined the transport of neutral quenchers in polyelectrolyte films using time-dependent fluorescence, 36,37 and other groups investigated the ion-permeability of MPFs using electrochemical techniques. 23,38-40 Ion transport through the membrane occurs through a set of tortuous pores with partitioning of ions through the bilayers of the film partially reponsible for rejection. The rate of ion diffusion through MPFs depends on ion charge, the number of bilayers in the film, charge density at the film surface, ionic strength, and individual bilayer thicknesses. Krasemann and Tieke recently showed that MPFs composed of 10-60 bilayers exhibit Cl<sup>-</sup>/SO<sub>4</sub><sup>2-</sup> selectivities as high as 45 in diffusion dialysis experiments, 15 and recent work in the Bruening group demonstrated that MPFs with as few as five bilayers can effectively cover porous supports. The selectivity of such ultrathin films depends greatly on the charge and composition of the MPF. 14,41-44 However, very little work has been performed using MPFs in NF. In one recent report, Krasemann and Tieke demonstrated that 60-bilayer films of poly(vinylamine)/poly(vinylsulfate) could reject 95% of NaSO<sub>4</sub> and up to 98% of MgSO<sub>4</sub>. However, in that case MPFs were quite thick, and water flux was several orders of magnitude lower than that of commercial NF membranes.

The goal of my research is to investigate the possibility of using alternating deposition procedure to create ultrathin NF membranes that will have greater efficiencies than current commercial membranes. Previous experiments have shown the ability of poly(styrene sulfonate) (PSS)/poly(allylamine hydrochloride) (PAH) ultrathin films to reject divalent ions in diffusion dialysis. <sup>14,41</sup> Based on these results, it may be possible to apply these MPFs to NF applications to allow for greater water flux values while exhibiting competitive ion rejection properties. Because of the ultrathin nature (<100 nm thick) of these PSS/PAH membranes, they should yield high water fluxes along with divalent ion rejection. My research also explores development of an industrially suitable support for MPFs and fouling of these membranes.

Chapter 2 of this thesis begins the discussion of MPF NF membranes by evaluating the NF performance of ultrathin PSS/PAH MPFs on alumina. Manipulation of deposition conditions and membrane composition allows control over membrane charge and affords Cl<sup>-</sup>/SO<sub>4</sub><sup>2-</sup> selectivities as high as 80. Additionally, these membranes permit water fluxes that are as much as twice as large as those of current commercial membranes. Typical water fluxes through commercial membranes are about 0.9 m<sup>3</sup>m<sup>-2</sup>m<sup>-1</sup>. <sup>45,46</sup>

In spite of the promise of these membranes, there are a number of challenges that must be overcome before they can be applied industrially. One

of these is the development of an inexpensive, porous substrate for film deposition. The porous alumina discs that I initially employed are very brittle and do not provide a high surface area. Although alumina tubes may be more robust and provide higher surface area, 47,48 those materials are still prohibitively expensive for large scale application. Most likely, the development of practical membrane systems will require replacement of alumina with a porous polymeric support. Chapter 3 describes my research in that direction. I deposited multilayer polyelectrolyte films on an ultrafiltration membrane and evaluated the NF performance of the system. Unfortunetly, membranes composed of 4.5bilayers of PSS/PAH on the ultrafiltration support, give fluxes that are considerably lower than those of similar membranes on alumina supports. Also the ion rejection decreased, leading me to believe that the film was not as thick as that on the alumina. This led to an investigation of the use of a non-selective, highly permeable gutter layer beneath the selective skin. Such a layer may allow full coverage of a polymeric support while maintaining the high flux and ion rejection of polyelectrolyte membranes.

Another major challenge in the development of any NF membrane is fouling, the deposition of insoluble material on the surface of the membrane. The presence of this unwanted material often decreases both flux and selectivity. This problem is complicated by the fact that there are a number of different fouling processes including deposition of natural organic matter (NOM),<sup>49-51</sup> colloidal fouling,<sup>52,53</sup> scaling,<sup>54</sup> and adsorption of proteins or bacteria.<sup>55,56</sup> The rates of the first three processes increase with both the roughness of the

membrane surface and permeate flux.<sup>53</sup> Colloidal and NOM fouling occur when insoluble particulates get caught in the hills and valleys of a rough surface, while scaling happens when cations and anions are rejected by the membrane such that they reach a surface concentration greater than the solubility of a particular salt. A common example of this is precipitation of calcium sulfate on membrane surfaces. All types of fouling lead to inefficiencies due to the formation of a cake layer on the surface of the membrane (Example shown in Figure 1.2). In order for polyelectrolyte NF membranes to become widely used commercially, these fouling issues must be explored, and methods for cleaning the membranes will likely need to be developed. Chapter 4 of this thesis suggests future work to determine the fouling rate of MPFs and potential methods for repairing fouled polyelectrolyte membranes.

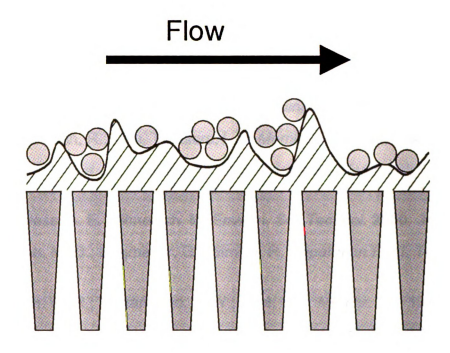


**Figure 1.2:** Cross-sectional view of a fouled membrane on a porous support. The circles represent colloids or NOM, which may get caught in the hills and valleys of a rough membrane surface to begin the formation of a cake layer.

#### References:

- (1) Xu, X.; Spencer, H. G. Desalination 1997, 114, 129.
- (2) Yaroshchuk, A.; Staude, E. *Desalination* **1992**, *86*, 115.
- (3) Hofman, J. A. M. H.; Beerendonk, E. F.; Folmer, H. C.; Kruithof, J. C. Desalination 1997, 113, 209.
- (4) Bohdziewicz, J.; Bodzek, M.; Wasik, E. Desalination 1999, 121, 139.
- (5) Berg, P.; Hagmeyer, G.; Gimbel, R. Desalination 1997, 113, 205.
- (6) Rautenbach, R.; Linn, T.; Eilers, L. *J. Membr. Sci.* **2000**, *174*, 231.
- (7) Bhattacharyya, D.; Williams, M. E. In *Membrane Handbook*; Ho, W. S. W., Sirkar, K. K., Eds.; Van Nostrand Reinhold: New York, 1992, pp 263.
- (8) Childress, A. E.; Elimelech, M. Environ. Sci. Technol. 2000, 34, 3710.
- (9) Afonso, M. D.; Hagmeyer, G.; Gimbel, R. Separation Purif. Technol. 2001, 22-23, 529.
- (10) Bowen, W. R.; Mohammad, A. W.; Hilal, N. J. Membr. Sci. 1997, 126, 91.
- (11) Kim, C. K.; Kim, J. H.; Roh, I. J.; Kim, J. J. *J. Membr. Sci.* **2000**, *165*, 189.
- (12) Košutic, K.; Kaštelan-Kunst, L.; Kunst, B. J. Membr. Sci. 2000, 168, 101.
- (13) Shibata, M.; Kobayashi, T.; Fujii, N. J. Appl. Polym. Sci. 2000, 75, 1546.
- (14) Harris, J. J.; Stair, J. L.; Bruening, M. L. Chem. Mater. 2000, 12, 1941.
- (15) Krasemann, L.; Tieke, B. *Langmuir* **2000**, *16*, 287.
- (16) Jin, W.; Toutianoush, A.; Tieke, B. *Langmuir* **2003**, *19*, 2550.
- (17) Dubas, S. T.; Farhat, T. R.; Schlenoff, J. B. *J. Am. Chem. Soc.* **2001**, *123*, 5368.
- (18) Lvov, Y. In *Protein Architecture*; Lvov, Y., Möhwald, H., Eds.; Marcel Dekker, Inc: New York, 2000, pp 125.
- (19) Schlenoff, J. B.; Ly, H.; Li, M. J. Am. Chem. Soc. 1998, 120, 7626.
- (20) Decher, G. Science 1997, 277, 1232.
- (21) Yoo, D.; Shiratori, S. S.; Rubner, M. F. *Macromolecules* **1998**, *31*, 4309.
- (22) Shiratori, S. S.; Rubner, M. F. *Macromolecules* **2000**, 33, 4213.
- (23) Harris, J. J.; Bruening, M. L. *Langmuir* **2000**, *16*, 2006.

- (24) Dubas, S. T.; Schlenoff, J. B. *Macromolecules* **1999**, 32, 8153.
- (25) Caruso, F.; Niikura, K.; Furlong, D. N.; Okahata, Y. *Langmuir* **1997**, *13*, 3422.
- (26) Decher, G.; Hong, J.-D.; Schmitt, J. Thin Solid Films 1992, 210/211, 831.
- (27) Hoogeveen, N. G.; Cohen Stuart, M. A.; Fleer, G. J. *Langmuir* **1996**, *12*, 3675.
- (28) Bertrand, P.; Jonas, A.; Laschewsky, A.; Legras, R. *Macromol. Rapid Commun.* **2000**, *21*, 319.
- (29) Kotov, N. A.; Dékány, I.; Fendler, J. H. J. Phys. Chem. 1995, 99, 13065.
- (30) Lvov, Y.; Haas, H.; Decher, G.; Möhwald, H. Langmuir 1994, 10, 4232.
- (31) Lvov, Y.; Ariga, K.; Ichinose, I.; Kunitake, T. *J. Am. Chem. Soc.* **1995**, *117*, 6117.
- (32) Wu, A.; Yoo, D.; Lee, J.-K.; Rubner, M. F. J. Am. Chem. Soc. 1999, 121, 4883.
- (33) Kotov, N. A.; Magonov, S.; Tropsha, E. Chem. Mater. 1998, 10, 886.
- (34) Leväsalmi, J.-M.; McCarthy, T. J. *Macromolecules* **1997**, *30*, 1752.
- (35) Stroeve, P.; Vasquez, V.; Coelho, M. A. N.; Rabolt, J. F. *Thin Solid Films* **1996**, *284-285*, 708.
- (36) Klitzing, R. v.; Möhwald, H. *Thin Solid Films* **1996**, 352.
- (37) Klitzing, R. v.; Möhwald, H. *Macromolecules* **1996**, 29, 6901.
- (38) Han, S.; Lindholm-Sethson, B. Electrochimica Acta 1999, 45, 845.
- (39) Farhat, T. R.; Schlenoff, J. B. Langmuir 2001, 17, 1184.
- (40) Farhat, T. R.; Schlenoff, J. B. J. Am. Chem. Soc. 2003, 125.
- (41) Stair, J. L.; Harris, J. J.; Bruening, M. L. Chem. Mater. 2001, 13, 2641.
- (42) Balachandra, A. M.; Dai, J.; Bruening, M. L. *Macromolecules* **2002**, *35*, 3171.
- (43) Dai, J.; Balachandra, A. M.; Lee, J. I.; Bruening, M. L. *Macromolecules* **2002**, *35*, 3164.
- (44) Dai, J.; Jensen, A. W.; Mohanty, D. K.; Erndt, J.; Bruening, M. L. *Langmuir* **2001**, *17*, 931.

- (45) Performance of commercially available membranes can be found at www.dow.com/liquidseps/pc/product.htm.
- (46) Bhattacharyya, D.; Williams, M. E.; Ray, R. J.; McCray, S. B. In *Membrane Handbook*; Ho, W. S. W., Sirkar, K. K., Eds.; Van Nostrand Reinhold: New York, 1992, pp 281.
- (47) Aust, U.; Moritz, T.; Popp, U.; Tomanal, G. J. Sol-Gel Sci & Tech. 2003, 26, 715.
- (48) Li, Y.; Wang, J.; Shi, J.; Zhang, X.; Lu, J.; Bao, Z. Sep. & Pur. Tech. 2003, 32, 397.
- (49) Cho, J.; Amy, G.; Pellegrino, J. Wat. Res. 1999, 33, 2517.
- (50) Yuan, W.; Zydney, A. L. Environ. Sci. Technol. 2000, 34, 5043.
- (51) Seidel, A.; Elimelech, M. J. Membr. Sci. 2002, 203, 245.
- (52) Zhu, X.; Elimelech, M. Environ. Sci. Technol. 1997, 31, 3654.
- (53) Vrijenhoek, E. M.; Hong, S.; Elimelech, M. J. Membr. Sci. 2001, 188, 115.
- (54) Le Gouellec, Y. A.; Elimelech, M. Env. Eng. Sci 2002, 19, 387.
- (55) Sadr Ghayeni, S. B.; Beatson, P. J.; Schneider, R. P.; Fane, A. G. *J. Membr. Sci.* **1998**, *138*, 29.
- (56) Pieracci, J. P.; Crivello, J. V.; Belfort, G. Chem. Mater. 2002, 14, 256.

#### Chapter 2

# NANOFILTRATION OF SALT SOLUTIONS USING MULTI-LAYERED POLYELECTROLYTE MEMBRANES ON ALUMINA SUPPORTS

Preparation of membranes using MPFs requires deposition of these films on a porous support, which provides mechanical strength. This chapter describes the NF performance of simple MPFs deposited on porous alumina (Anodisc™) substrates, while Chapter 3 focuses on polymeric supports. Porous alumina supports are ideal for initial NF studies because they have a well-defined, highly porous structure that allows a very high water flux. This enables the study of flux and rejection properties of the MPFs with minimal effects from the support. Additionally, below pH 8 alumina disks have a positively charged surface¹ that allows for polyelectrolyte deposition, and the small diameter of surface pores (20 nm) easily permits full coverage of the support without filling of the pores.¹

The main parameters of importance in nanofiltration are water permeance and ion rejection. Recently, Jin and coworkers examined NF with 60-bilayer poly(vinylamine)/poly(vinylsulfate) films,<sup>2</sup> but water flux through those membranes was very low. In contrast, the minimal thicknesses of the MPFs employed in this work allow water fluxes comparable to those achieved with commercial membranes. Additionally, this study shows that ion rejection can be manipulated by altering the outer polyelectrolyte layer to change packing and surface charge. Such manipulations afford enhancements in Cl<sup>-</sup>/SO<sub>4</sub><sup>2-</sup> selectivities that occur without an accompanying decrease in Cl<sup>-</sup> flux. Our

studies of NF with both mixed and single-salt solutions suggest that selectivity is a complicated function of solution composition, surface charge, packing, and ion adsorption.

#### **Experimental**

#### Materials

Poly(allylamine hydrochloride) (PAH) (Aldrich, M<sub>w</sub>=70,000), poly(styrene sulfonate) sodium salt (PSS) (Aldrich, M<sub>w</sub>=70,000), poly(acrylic acid) (PAA) (M<sub>w</sub>=90,000, 25 wt% solution, Alfa Aesar), MnCl<sub>2</sub> (Acros), NaBr (Aldrich), NaCl (Spectrum and CCl), CaCl<sub>2</sub> (CCl), Na<sub>2</sub>SO<sub>4</sub> (Baker), MgSO<sub>4</sub>•7H<sub>2</sub>O (Spectrum), NaHCO<sub>3</sub> (Mallinckrodt), Na<sub>2</sub>CO<sub>3</sub> (Spectrum), CaSO<sub>4</sub> (CCl), 3-mercaptopropionic acid (MPA) (Aldrich), mesityl oxide (Aldrich) and Congo Red (Fisher) were used as received.

### Polyelectrolyte Deposition on Porous Alumina Supports

Prior to film deposition, the porous alumina supports (Whatman<sup>®</sup> Anodisc™ 0.02 µm membrane filters) were UV/O<sub>3</sub> cleaned for 15 minutes (Boekel UV\_Clean™ model 135500). The alumina membrane has two distinct sides: the filtrate side, which has a skin layer of 0.02 µm-diameter pores, and the permeate side, which has 0.2 µm-diameter pores. The polyelectrolyte deposition was limited to the filtrate side using a holder. Polyelectrolyte deposition began with a 2-min immersion of the alumina support in a 0.02 M solution of PSS. Polymer molarities are given with respect to the repeating unit. The PSS solution

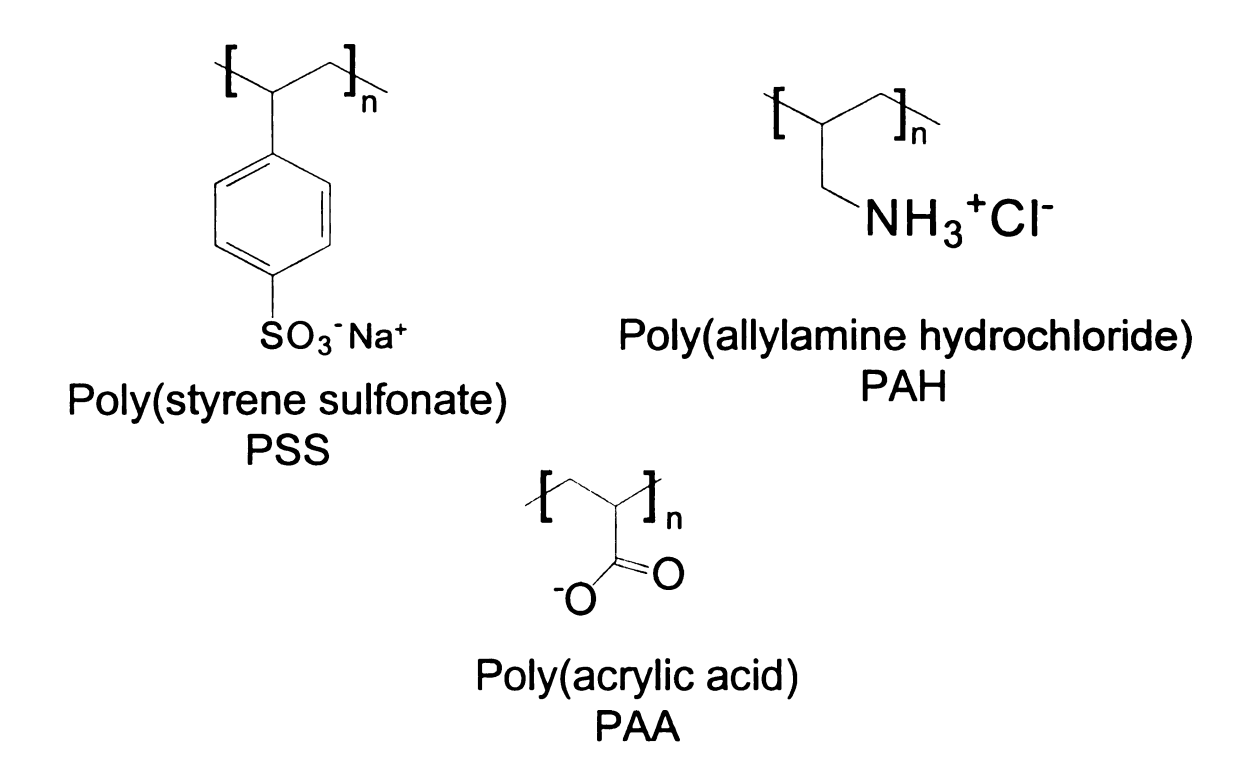


Figure 2.1: The chemical structures of the polyelectrolytes used in this study.

contained 0.5 M MnCl<sub>2</sub> and was adjusted to pH 2.1 with HCl. Following a 1-min water rinse, the support was then immersed for 5 min in a 0.02 M PAH solution that contained 0.5 M NaBr (pH adjusted to 2.3 with HCl). Subsequent bilayers were deposited in the same way. Deposition conditions were chosen based on literature preparations of polyelectrolyte films, 3-6 and immersion times are not necessarily sufficient to achieve equilibrium adsorption.<sup>3-6</sup> In some cases, after deposition of 4-bilayers of PSS/PAH, the membranes were immersed in a PSS solution that contained 0 or 2.5 M MnCl<sub>2</sub>. Another group of membranes had 1 layer of PAA deposited on 4-bilayers of PSS/PAH (PAA deposition: immersion in a 0.02 M PAA solution containing 0.5 M NaCl and adjusted to pH 4.5 with NaOH). A 1-minute rinse with water (Milli-Q, 18 MΩ-cm) followed all polyelectrolyte deposition steps. After deposition of the desired number of polyelectrolyte layers, membranes were stored in water until use. membranes were dried before use, and there was no noticeable difference in performance after drving.

#### Ellipsometry

Ellipsometric thickness determinations (J.A. Woollam model M-44 rotating analyzer ellipsometer) were performed using Au-coated substrates (200 nm of Au sputtered on 20 nm of Cr on Si(100) wafers) that were treated with 0.002 M 3-mercaptopropanoic acid (MPA) in ethanol for 30 minutes and rinsed with ethanol. This process primes the surface with –COOH groups that can be ionized for subsequent polycation deposition. Formation of films on these substrates was

accomplished using the same deposition conditions as with alumina supports, but PAH was deposited first rather than PSS. Prior to film deposition, optical constants of the MPA-coated substrates were determined at the 44 wavelengths of the ellipsometer, and for calculation of MPF thickness, the refractive index of the MPF was assumed to be 1.5.<sup>7,8</sup> The thickness of the top PSS layer was determined as the difference between film thicknesses after deposition of 4.5 and 5 PAH/PSS bilayers. Previous work showed that films on Au and porous alumina have similar thicknesses.<sup>1</sup>

#### **Nanofiltration**

NF experiments were conducted in the home-built, cross-flow system shown schematically in Figure 2.2. The system was pressurized to 4.8 bar with Ar, and the feed tank was used to store the various brine solutions (4 L), which contained 50 or 1000 ppm of Na<sup>+</sup>, SO<sub>4</sub><sup>2-</sup>, Ca<sup>2+</sup>, or Mg<sup>2+</sup>. Solutions were prepared from NaCl, Na<sub>2</sub>SO<sub>4</sub>, CaCl<sub>2</sub>, and MgSO<sub>4</sub>, respectively. A stainless steel frit (Mott Corporation) was used as a prefilter to remove rust or particulate matter from the feed stream. The flow meter was set to 18 mL/min, which is 100-fold greater than the permeate flow rate. This cross flow is high enough to minimize concentration polarization, as increasing the cross flow rate to 40 mL/min had little, if any, effect on ion rejection or permeate flux. The membranes were housed in a home-built stainless steel/o-ring cell that exposed an active membrane area of 1.5 cm<sup>2</sup> (Figure 2.3). The active area was determined by

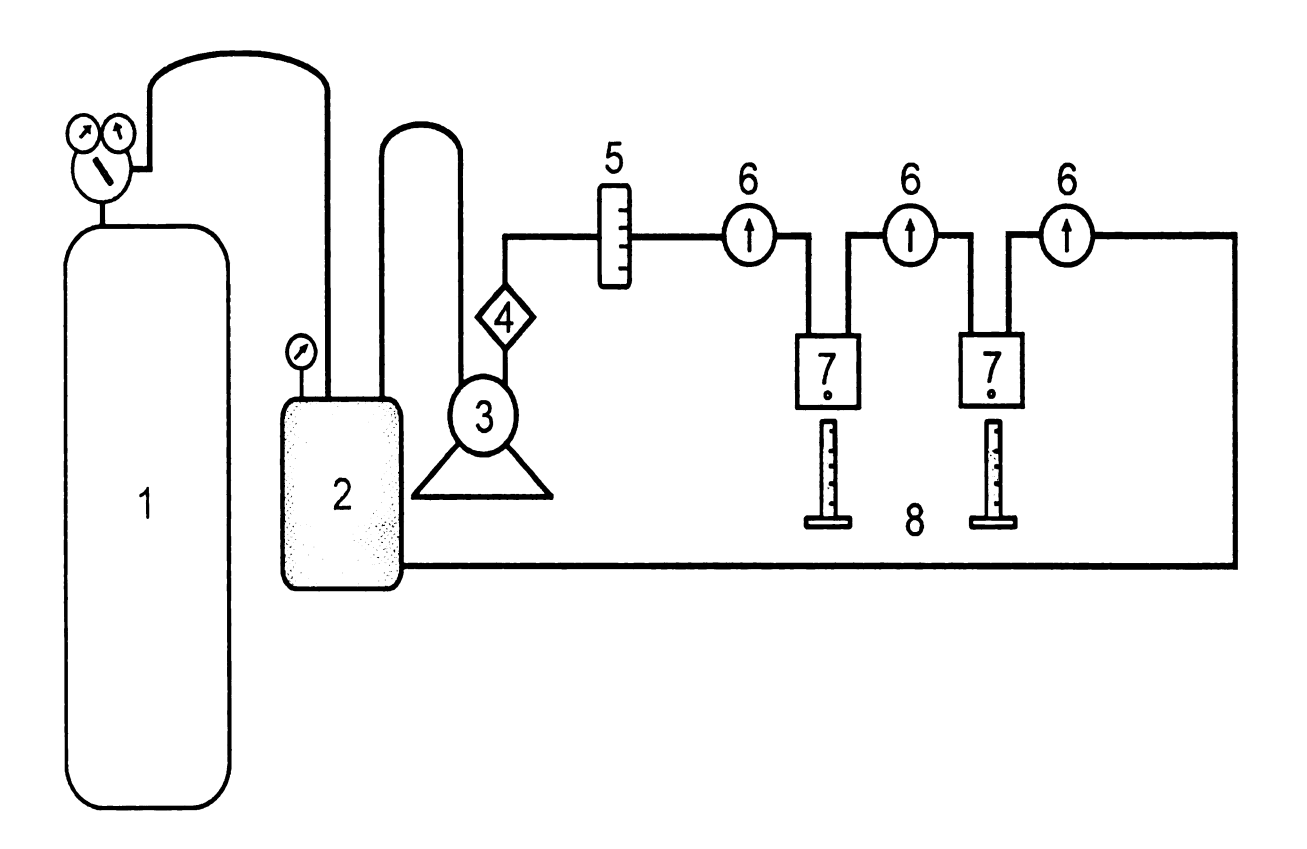


Figure 2.2: Experimental setup for nanofiltration experiments: Ar tank (1), stainless steel feed tank (2), centrifugal pump (3), prefilter (4), flowmeter (5), pressure gauges (6), membrane cells (7), and graduated cylinders (8). There is a water bath between the pump and the flow meter to dissapate heat from the pump and prefilter. (Figure courtesy of Jeremy Harris)

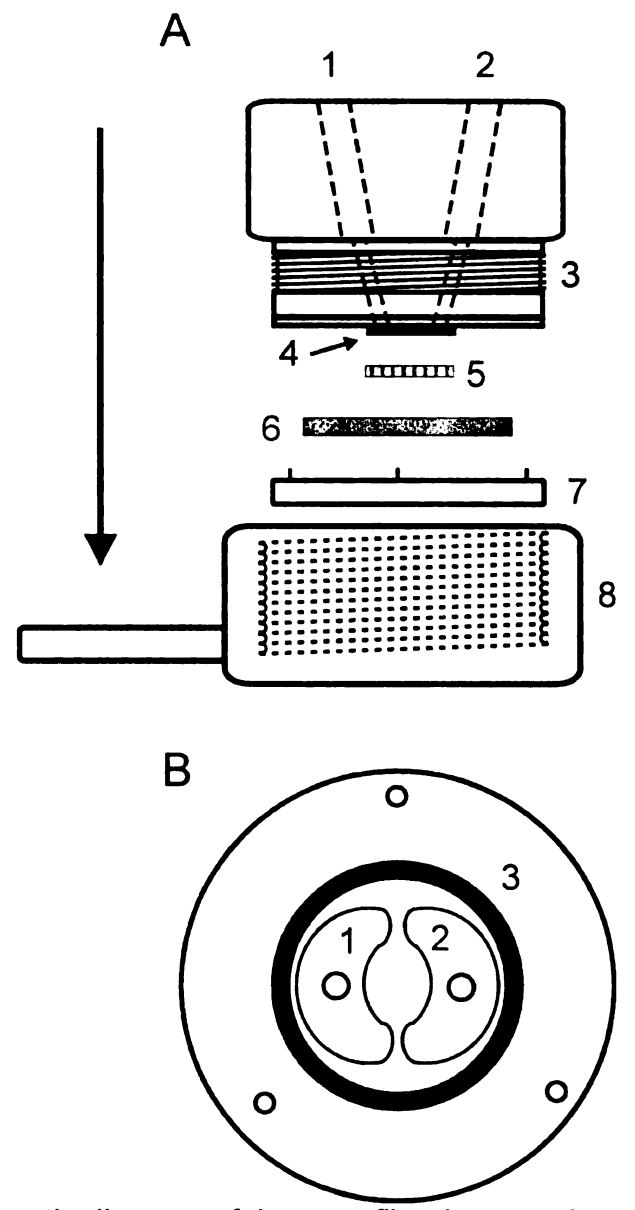


Figure 2.3: Schematic diagram of the nanofiltration membrane cell. (A) shows how the cell is placed together: inlet/outlet ports (1&2), threads (3), rubber o-ring (4), membrane being analyzed (5), porous stainless steel frit (6), cap that holds the frit and presses the membrane tight against o-ring (7), and threaded bottom part of cell that top part screws into (8). The cell is assembled in the direction of the arrow. (B) shows a bottom view of the upper portion of the cell: recessed inlet/outlet channels (1&2) and o-ring (3). (Figure courtesy of Jeremy Harris)

performing NF with 0.1% congo red dye, and then measuring the diameter of the stained area of the membrane with calipers. Pressure gauges were used to ensure that no significant pressure drops occurred across the membrane cells. Salt rejection in single-salt NF experiments was determined using conductivity measurements and appropriate calibration curves.

Once the system was pressurized, the membranes were allowed to be in contact with the flowing solution for 60 min, and permeate aliquots were collected every 30 min for 1.5 h. After a total of 18 h of pressurized operation, permeate aliquots were again collected every 30 min for three hours. The 18-h conditioning period is sufficient to achieve stable membrane performance. In some cases, NF was performed for 48 h, and no significant change in flux or rejection relative to that after 18 h was noticed. These results demonstrate that no significant delamination of the polyelectrolyte layers occurs over short time periods.

# Cl<sup>-</sup>/SO<sub>4</sub><sup>2-</sup> selectivity measurements

Solutions with both Cl<sup>-</sup> and SO<sub>4</sub><sup>2-</sup> (sodium salts) were prepared at anion concentrations of 50 or 1000 ppm. NF with these solutions occurred as described above, and ion concentrations were determined with a Dionex 600 ion chromatograph using an AS14A anion column and an 8 mM Na<sub>2</sub>CO<sub>3</sub>/1 mM NaHCO<sub>3</sub> eluent. The concentrations were determined using a set of five standards bracketing the expected feed and permeate concentrations.

#### Capillary Electrophoresis

Capillary electrophoresis experiments were performed with an Agilent G1600A instrument that employed a UV/Visible detector. Bare silica capillaries (100 µm inside diameter, purchased from BIOTAQ) were first treated with 0.1 M NaOH for 30 min and rinsed with water for 5 min. The first PAH layer was deposited onto the inside of the silica column by passing a PAH solution through the capillary for 10 min using a pressure-driven (950 mbar) water flow. All subsequent PAH and PSS layers were deposited with 5-min flows using the solutions described previously. The capillary was rinsed with water for 5 min between each step. Mesityl oxide (500 ppm) was used as a marker to detect electroosmotic flow. Flow experiments with 1000 ppm SO<sub>4</sub><sup>2-</sup> were performed using a potential of 15 kV in positive mode, while experiments with 1000 ppm Ca<sup>2+</sup> utilized 5 kV in negative mode.

#### **Results and Discussion**

#### Single-salt Nanofiltration with PSS/PAH Membranes

One of the main advantages of MPFs in NF is their small thickness, which should result in high water fluxes. However, to achieve high rejections of analyte molecules along with high water permeabilities, MPFs must be thick enough to completely cover the pores of the material on which they are deposited. Our previous studies showed that full coverage of a porous alumina support (0.02 µm-diameter surface pores) by a PSS/PAH film requires adsorption of at least 4.5 bilayers.<sup>1,9</sup> Therefore, NF experiments focused on films consisting of 4.5 or 5

PSS/PAH bilayers. Films with 4.5 bilayers terminate in a PSS layer ([PSS/PAH]<sub>4</sub>PSS), while 5-bilayer films terminate with PAH ([PSS/PAH]<sub>5</sub>). Both ellipsometric studies and scanning electron microscope images indicate that 4.5-bilayer PSS/PAH films have thicknesses of ~20 nm.<sup>1,7</sup> In NF experiments, coverage of porous alumina by PSS/PAH is evident from a dramatic decrease in water flux after deposition of 4.5-bilayers. Under 4.8 bar of pressure, water flux through the bare alumina membrane is about 180 m³m-²d-¹, but after PSS/PAH deposition, the flux decreases to between 1 and 2.3 m³m-²d-¹ (Tables 2.1 & 2.2). Fluxes through PSS/PAH films are comparable to those of commercial NF membranes. <sup>10,11</sup>

In most cases, the water flux decreases with an increasing salt concentration (compare Tables 2.1 and 2.2), presumably because of increased osmotic pressure. Calculated osmotic pressures for 1000 ppm Mg<sup>2+</sup> (MgSO<sub>4</sub>), Ca<sup>2+</sup> (CaCl<sub>2</sub>), SO<sub>4</sub><sup>2-</sup> (Na<sub>2</sub>SO<sub>4</sub>), and Na<sup>+</sup> (NaCl) are 2.0, 1.8, 0.75, and 2.1 bar, respectively, for 100% rejection. Water flux with 1000 ppm Na<sup>+</sup> is similar to that with 50 ppm Na<sup>+</sup>, but in this case, osmotic pressure effects are minimized by low rejections. Increased adsorption of ions in the polyelectrolyte membrane at higher ionic strength (see below) could also affect water flux.

PSS/PAH membranes show impressive ion-rejection values that vary with the charge of the outer layer of the membrane. As seen in the top two rows of Table 2.1, ion-rejection increases when the outer layer charge matches the charge of the divalent ion of a 2:1 salt. For example, CaCl<sub>2</sub> rejection increases from approximately 86% to 96% after deposition of a terminating PAH layer. The

opposite trend occurs for Na<sub>2</sub>SO<sub>4</sub>. This suggests that electrostatic (Donnan) exclusion plays a major role in salt rejection. 12 One would expect little dependence of NaCl or MgSO<sub>4</sub> rejection on the charge of the outer layer of the membrane because the cations and anions in these salts have the same magnitude of charge. However, rejection of NaCl increases on going from a 4.5bilayer to a 5-bilayer PSS/PAH membrane. The higher NaCl rejection of 5bilayer membranes is accompanied by a 40% decrease in water flux relative to This decrease is not simply due to increased film 4.5-bilayer membranes. thickness, as water flux through a 5.5-bilayer film is still 30% higher than that for a 5-bilayer membrane. The lower water flux and higher NaCl rejection of membranes terminated with PAH suggest that the PAH surface layer is more dense than PSS. In the case of MgSO<sub>4</sub>, water flux is nearly the same for 4.5and 5-bilayer PSS/PAH membranes, probably because of Mg<sup>2+</sup> adsorption to the PSS layer. This adsorption may equalize MgSO<sub>4</sub> rejection by PSS- and PAHterminated films.

Adsorption of divalent ions may also explain why MgSO<sub>4</sub>, Na<sub>2</sub>SO<sub>4</sub>, and CaCl<sub>2</sub> rejections do not vary greatly with electrolyte concentration (compare Tables 2.1 and 2.2, rows 1 and 2).<sup>13,14</sup> Increased adsorption of divalent ions at higher electrolyte concentrations should enhance electrostatic exclusion by increasing membrane charge. This effect may compensate the greater screening of surface charge that should occur at higher ionic strengths. NaCl rejection does increase with decreasing concentration, suggesting that adsorption of monovalent ions is minimal. The high CaCl<sub>2</sub> rejection by 4.5-bilayer

**Table 2.1:** Ion rejection (percent) and water flux values (listed in parentheses in m<sup>3</sup>m<sup>-2</sup>d<sup>-1</sup>) for various polyelectrolyte nanofiltration membranes. The salt solutions were 1000 ppm in the ion of interest, and nanofiltration was performed at 4.8 bar.

Membrane	Na <sup>+</sup> (NaCl)	SO <sub>4</sub> <sup>2-</sup> (Na <sub>2</sub> SO <sub>4</sub> )	Ca <sup>2+</sup> (CaCl <sub>2</sub> )	Mg <sup>2+</sup> (MgSO <sub>4</sub> )
[PSS/PAH] <sub>4</sub> PSS*	29±5	56±8	86±2	96±1
	(2.2±0.3)	(1.6±0.1)	(1.5±0.3)	(1.2±0.2)
[PSS/PAH]₅	43±6	35±5	96.0±0.6	96±1
	(1.4±0.1)	(1.0±0.0)	(1.1±0.1)	(1.1±0.2)
[PSS/PAH]₄PSS**	28±7	53±9	91±1	95±2
	(2.1±0.1)	(1.5±0.1)	(1.1±0.3)	(1.2±0.2)
[PSS/PAH] <sub>4</sub> PSS***	13±2	95±2	48±8	90±1
	(2.5±0.2)	(1.8±0.2)	(1.5±0.6)	(1.0±0.2)
[PSS/PAH]₄PAA	24±2	92±4	85±2	94±1
	(1.1±0.1)	(1.0±0.1)	(1.1±0.1)	(0.9±0.1)

<sup>\* 0.5</sup> M MnCl<sub>2</sub> in final PSS layer deposition solution

<sup>\*\* 0</sup> M MnCl<sub>2</sub> in final PSS layer deposition solution

<sup>\*\*\* 2.5</sup> M MnCl<sub>2</sub> in final PSS layer deposition solution

**Table 2.2:** Ion rejection (percent) and water flux values (listed in parentheses in m<sup>3</sup>m<sup>-2</sup>d<sup>-1</sup>) for various polyelectrolyte nanofiltration membranes. The salt solutions were 50 ppm in the ion of interest, and nanofiltration was performed at 4.8 bar.

Membrane	Na <sup>+</sup> (NaCl)	SO <sub>4</sub> <sup>2-</sup> (Na <sub>2</sub> SO <sub>4</sub> )	Ca <sup>2+</sup> (CaCl <sub>2</sub> )	Mg <sup>2+</sup> (MgSO₄)
[PSS/PAH] <sub>4</sub> PSS*	60±7	44±7	94±1	96+1
	(2.0±0.5)	(2.1±0.3)	(2.3+0.3)	(1.6+0.1)
[PSS/PAH]₅	81±3	42±5	96.6±0.7	97.6±0.5
	(1.1±0.2)	(1.3±0.0)	(1.4±0.1)	(1.7±0.1)
[PSS/PAH] <sub>4</sub> PSS**	51±6	48±3	94±1	94±2
	(2.2±0.2)	(1.9±0.2)	(2.0±0.1)	(1.8±0.4)
[PSS/PAH] <sub>4</sub> PSS***	31.0±5	91±4	64±7	88±5
	(2.1±0.2)	(1.7±0.1)	(1.7±0.1)	(1.5±0.3)
[PSS/PAH]₄PAA	45±6	70±8	87±2	96±2
	(1.2±0.1)	(1.0±0.1)	(1.4±0.1)	(1.4±0.1)

<sup>\* 0.5</sup> M MnCl<sub>2</sub> in final PSS layer deposition solution

<sup>\*\* 0</sup> M MnCl<sub>2</sub> in final PSS layer deposition solution

<sup>\*\*\* 2.5</sup> M MnCl<sub>2</sub> in final PSS layer deposition solution

PSS/PAH membranes also provides evidence for ion adsorption. Calcium ions should not be rejected by the negative surface presented by PSS-terminated films, but rejection is about 90%, suggesting that adsorption of Ca<sup>2+</sup> creates a positively charged surface. It should be noted, however, that high Ca<sup>2+</sup> rejections may be partly due to large size of this ion. The hydrated radius of Ca<sup>2+</sup> is 271 pm, while that of Na<sup>+</sup> is 228 pm.<sup>15</sup>

To confirm that adsorption of divalent ions occurs, we performed measurements of electroosmotic flow in silica capillaries coated with PAH/PSS films. <sup>16,17</sup> For films terminated with PSS (5 PAH/PSS bilayers), electroosmotic flow moves toward the negative electrode when the electrolyte contains 1000 ppm SO<sub>4</sub><sup>2-</sup> (Na<sub>2</sub>SO<sub>4</sub>). However, when the electrolyte contains 1000 ppm Ca<sup>2+</sup> (CaCl<sub>2</sub>), a negative potential had to be applied in order to get the mesityl oxide off the column. This shows that the direction of electroosmotic flow reverses, confirming Ca<sup>2+</sup> adsorption.

#### Controlling Rejection by Manipulating the Outer Polyelectrolyte Layer

The results given above indicate that charge at the membrane-solution interface plays a major role in ion rejection by MPFs. One way to control the charge density at this interface is to vary the amount of supporting electrolyte in the polyelectrolyte deposition solution. High concentrations of salts electrostatically screen charged groups in the polymer, leading to a film with increased thickness and a more loopy structure. <sup>13,18,19</sup> In general, increasing the supporting electrolyte concentration present during deposition of the outer

polyelectrolyte layer should yield a higher density of fixed charge at the MPF surface. When the outer layer is thick and has a loopy structure, its surface is less intermingled with underlying layers and thus has a higher net charge density. To examine the effect of supporting electrolyte, a 4-bilayer PSS/PAH film was prepared, as described in the experimental section, and subsequently capped with a final layer of PSS that was deposited from solutions containing various amounts of MnCl<sub>2</sub>. Ellipsometric measurements with films deposited on Au yielded PSS capping layer thicknesses of 21±3, 28±3, and 51±7 Å for films deposited in the presence of 0, 0.5, and 2.5 M MnCl<sub>2</sub>, respectively. These thicknesses are consistent with literature values. As a loopy structure, its extraction of the MPF surface is the MPF surface.

Tables 2.1 and 2.2 show that ion rejection depends significantly on the concentration of supporting electrolyte present during the deposition of the outer polyelectrolyte layer. For both 50 and 1000 ppm  $SO_4^{2-}$ ,  $Na_2SO_4$  rejections increase from about 50% to >90% when the concentration of  $MnCl_2$  present during deposition of the PSS capping layer increases from 0 to 2.5 M. Remarkably, this increase in rejection occurs with no substantial change in water flux. In contrast to  $Na_2SO_4$ ,  $CaCl_2$  and  $MgSO_4$  rejections decrease when the top PSS layer is deposited from 2.5 M rather than 0 M  $MnCl_2$ . All of the ion-rejection results are consistent with increased negative surface charge due to the presence of 2.5 M  $MnCl_2$  during PSS deposition.  $MnCl_2$  was chosen as a supporting electrolyte because it provides a high ionic strength, but one concern in utilizing this salt is that adsorption of  $Mn^{2+}$  could affect membrane properties.

However, high water flux and rejection of negatively charged anions suggest that any Mn<sup>2+</sup> adsorbed in the membrane is removed during rinsing or NF.

Another way to control surface charge is to change the composition of the polyanion (or polycation) used to cap the membrane. Previous studies suggest that the high charge density of PAA-capped 4-bilayer PSS/PAH films should increase SO<sub>4</sub><sup>2-</sup> rejection relative to that seen with 4.5-bilayer PSS/PAH films.<sup>9</sup> Tables 2.1 and 2.2 show that films capped with PAA do exhibit increased SO<sub>4</sub><sup>2-</sup> rejection compared to 4.5-bilayer PSS/PAH membranes (PSS capping layer deposited in the presence of 0 or 0.5 M MnCl<sub>2</sub>). However, the high density of the PAA layer also results in decreased water fluxes.

### Cl<sup>-</sup>/SO<sub>4</sub><sup>2-</sup> Selectivity of PSS/PAH membranes

To further investigate the selectivity of PSS/PAH membranes, NF was performed with solutions containing both NaCl and Na<sub>2</sub>SO<sub>4</sub>. Table 2.3 contains NF results for 50 ppm Cl<sup>-</sup>/50 ppm SO<sub>4</sub><sup>2-</sup> and 1000 ppm Cl<sup>-</sup>/1000 ppm SO<sub>4</sub><sup>2-</sup> feed solutions. In nearly every case, Cl<sup>-</sup> rejection decreases compared to single-salt experiments, while SO<sub>4</sub><sup>2-</sup> rejection increases. In some cases, the concentration of Cl<sup>-</sup> in the permeate even exceeds the concentration of Cl<sup>-</sup> in the feed. This occurs because the concentration of Na<sup>+</sup> in the mixed feed solutions is greater than that of Cl<sup>-</sup>, and thus diffusive flux of Na<sup>+</sup> is greater than that of Cl<sup>-</sup>. The difference in diffusive fluxes results in a diffusion potential that enhances Cl<sup>-</sup> transport. In solutions containing only Na<sub>2</sub>SO<sub>4</sub>, a diffusion potential that enhances the SO<sub>4</sub><sup>2-</sup> flux also develops because the diffusivity of Na<sup>+</sup> in the

membrane is much greater than that of  $SO_4^{2-}$ . The presence of  $Cl^-$  in the mixed salt solutions reduces this diffusion potential, and thus,  $SO_4^{2-}$  rejection increases in mixed solutions.  $Cl^-/SO_4^{2-}$  selectivities were calculated according to equation 1, where  $C^p$  and  $C^f$  represent the concentrations of the analyte in the permeate and the feed, respectively.

Selectivity = 
$$(C_{CC}^p / C_{CC}^f)/(C_{SO_c^{2-}}^p / C_{SO_c^{2-}}^f)$$
 (1)

For single-salt solutions, this selectivity can be rewritten as equation 2, where %R represents the percent rejection of the appropriate salt.

Selectivity = 
$$(100-\% R_{NaCl})/(100-\% R_{Na,SOL})$$
 (2)

Table 2.4 shows that in all cases, Cl<sup>-</sup>/SO<sub>4</sub><sup>2-</sup> selectivities are higher with mixed salt solutions, presumably because of diffusion potentials, as mentioned above. Additionally, selectivities depend greatly on the outer polyelectrolyte layer. Deposition of the final layer of PSS from 2.5 M MnCl<sub>2</sub>, rather than 0.5 M MnCl<sub>2</sub>, increases selectivity to approximately 30 (a 5 to 10-fold increase) for both 50 ppm and 1000 ppm mixed solutions.

Along with high selectivity, practical Cl<sup>-</sup>/SO<sub>4</sub><sup>2-</sup> separations will require both high water flux and low Cl<sup>-</sup> rejections. Remarkably, the increase in selectivity due to the presence of 2.5 M MnCl<sub>2</sub> in the PSS deposition solution is not accompanied by a decrease in water flux. Additionally, the low Cl<sup>-</sup> rejections by these films (-6 and 40%) could allow a high recovery of NaCl. All films with SO<sub>4</sub><sup>2-</sup> rejections greater than 90% showed Cl<sup>-</sup> rejections of 40% or lower.

Termination of membranes with PAA rather than PSS also yields very high selectivities. With a 50 ppm mixed solution, PAA-capped membranes show a

**Table 2.3:** Percent rejection values for individual anions and water fluxes (in m³m-2d-1) from NF experiments with mixed salt solutions.

	50 ppm Cl <sup>-</sup> /50 ppm SO <sub>4</sub> <sup>2-</sup>			1000	ppm Cl <sup>-</sup> /10 SO <sub>4</sub> <sup>2-</sup>	00 ppm
Membrane	Cl <sup>-</sup>	SO <sub>4</sub> <sup>2</sup> -	water flux	Cl <sup>-</sup>	SO <sub>4</sub> <sup>2-</sup>	water flux
[PSS/PAH]₄PSS (final layer from 0.5 M MnCl₂)	9±6	73±6	1.6±0.1	-2±5	81±8	1.3±0.2
[PSS/PAH]₄PSS (final layer from 2.5 M MnCl₂)	40±8	98±1	1.8±0.2	-6±1	97±1	1.8±0.3
[PSS/PAH]₄PAA	17±3	95±2	1.0±0.1	5±1	98.9±0.1	0.9±0.1

**Table 2.4:** Cl<sup>-</sup>/SO<sub>4</sub><sup>2-</sup> selectivities for single-salt and mixed-salt (value in parentheses) NF experiments. These values were calculated from the average % rejections shown in Tables 1, 2, and 3. Solutions were prepared using NaCl and Na<sub>2</sub>SO<sub>4</sub>.

Membrane	50 ppm Cl <sup>-*</sup> /50 ppm SO <sub>4</sub> <sup>2-</sup>	1000 ppm Cl <sup>-*</sup> /1000 ppm SO <sub>4</sub> <sup>2-</sup>
[PSS/PAH] <sub>4</sub> PSS (final layer from	0.7 ±0.1	1.6±0.4
0.5 M MnCl <sub>2</sub> )	(3.5±0.6)	(6±3)
[PSS/PAH] <sub>4</sub> PSS (final layer from	7.7±1.3	17.4±2.7
2.5 M MnCl <sub>2</sub> )	(28±5)	(33±8)
[PSS/PAH]₄PAA	1.8±0.3	9.5±0.2
[F33/FAN]4FAA	(16±4)	(84±4)

<sup>\*</sup>Single-salt data for chloride-containing solutions (NaCl) were actually measured using 50 ppm or 1000 ppm Na<sup>+</sup> (Tables 1 and 2). Thus, for single-salt measurements, Cl<sup>-</sup> concentration was 77 or 1540 ppm.

Cl<sup>-</sup>/SO<sub>4</sub><sup>2-</sup> selectivity of about 16, but when Cl<sup>-</sup> and SO<sub>4</sub><sup>2-</sup> concentrations are 1000 ppm, selectivity increases to 84. This result parallels single-salt experiments, but overall selectivities are much larger. However, water flux through PAA-capped membranes is only ~60% of that through PSS/PAH.

In most solutions found in nature, the amount of Cl<sup>-</sup> would be much greater than that of SO<sub>4</sub><sup>2-</sup>. To simulate such a situation, we performed NF experiments with 1000 ppm Cl<sup>-</sup>/50 ppm SO<sub>4</sub><sup>2-</sup> solutions using a PSS/PAH membrane capped with PSS deposited from 2.5 M MnCl<sub>2</sub>. Selectivity in this case is 20 and Cl<sup>-</sup> rejection is 20%. Selectivity is only slightly lower than that found for 50 ppm Cl<sup>-</sup>/50 ppm SO<sub>4</sub><sup>2-</sup> solutions.

#### Conclusions

Alternating polyelectrolyte adsorption on porous supports is a convenient, versatile method for constructing NF membranes. These membranes provide high water fluxes and rejections of divalent ions along with Cl<sup>-</sup>/SO<sub>4</sub><sup>2-</sup> selectivities as high as 80. Electrostatic exclusion is a major factor in transport selectivity, and thus, by changing the outer layer charge in PSS/PAH membranes, rejection, flux, and selectivity can be tailored to fit the needs of a particular separation. These attributes make MPFs potentially attractive for NF applications such as water and salt purification.

#### References

- (1) Harris, J. J.; Stair, J. L.; Bruening, M. L. Chem. Mater. 2000, 12, 1941.
- (2) Jin, W.; Toutianoush, A.; Tieke, B. *Langmuir* **2003**, *19*, 2550.
- (3) Caruso, F.; Niikura, K.; Furlong, D. N.; Okahata, Y. *Langmuir* **1997**, *13*, 3422.
- (4) Decher, G.; Lvov, Y.; Schmitt, J. *Thin Solid Films* **1994**, *244*, 772.
- (5) Yoo, D.; Shiratori, S. S.; Rubner, M. F. *Macromolecules* **1998**, *31*, 4309.
- (6) Casson, J. L.; Wang, H.-L.; Roberts, J. B.; Parikh, A. N.; Robinson, J. M.; Johal, M. S. *J. Phys. Chem. B* **2002**, *106*, 1697.
- (7) Harris, J. J.; Bruening, M. L. *Langmuir* **2000**, *16*, 2006.
- (8) Tronin, A.; Lvov, Y.; Nicolini, C. Colloid Polym. Sci. 1994, 272, 1317.
- (9) Stair, J. L.; Harris, J. J.; Bruening, M. L. Chem. Mater. 2001, 13, 2641.
- (10) Performance of commercially available membranes can be found at www.dow.com/liquidseps/pc/product.htm.
- (11) Bhattacharyya, D.; Williams, M. E.; Ray, R. J.; McCray, S. B. In *Membrane Handbook*; Ho, W. S. W., Sirkar, K. K., Eds.; Van Nostrand Reinhold: New York, 1992, pp 281.
- (12) Peeters, J. M. M.; Boom, J. P.; Mulder, M. H. V.; Strathmann, H. *J. Membr. Sci.* **1998**, *145*, 199.
- (13) Schlenoff, J. B.; Ly, H.; Li, M. J. Am. Chem. Soc. **1998**, *120*, 7626.
- (14) Toutianoush, A.; Tieke, B. Mat. Sci. and Eng. C 2002, 22, 135.
- (15) Marcus, Y. *Biophysical Chemistry* **1994**, *51*, 111.
- (16) Graul, T. W.; Schlenoff, J. B. Anal. Chem. 1999, 71, 4007.
- (17) Capillary Electrophoresis measurements kindly done by Matt Miller.
- (18) Shubin, V.; Linse, P. J. Phys. Chem. **1995**, 99, 1285.
- (19) Steeg, H. G. M. v. d.; Stuart, M. A. C.; Keizer, A. d.; Bijsterbosch, B. H. *Langmuir* **1992**, *8*, 2538.

- (20) Phuvanartnuruks, V.; McCarthy, T. J. Macromolecules 1998, 31, 1906.
- (21) Farhat, T. R.; Schlenoff, J. B. *Langmuir* **2001**, *17*, 1184.
- (22) Schlenoff, J. B.; Dubas, S. T. *Macromolecules* **2001**, *34*, 592.

#### **Chapter 3**

## Development of Composite Polyelectrolyte NF Membranes on Polymeric Supports

High throughput applications of filtration membranes, *e.g.*, NF, generally utilize spirally wound or hollow fiber membranes that offer higher surface areas and, hence, higher fluxes than sheet membranes. Such membrane geometries are not practicle with ceramic materials, so polymers such as polysulfone are usually employed as skin layer supports. In addition to being more flexible than ceramics, polymeric supports are also much less expensive. This chapter describes our initial investigations of MPF deposition on porous polymer substrates and the NF properties of the resulting composite membranes.

Any material employed as a support in a composite MPF membrane must permit high water flux while having pore sizes small enough to be coated by an ultrathin polyelectrolyte film. Ultrafiltration membranes may be capable of fulfilling both of these requirements. Figure 3.1 shows that pores in a Pall Corporation 100 kD ultrafiltration membrane have diameters ranging from 45 to 70 nm. Although these pores are 2 to 4 times larger than those in the alumina substrates described in Chapter 2, they still may be small enough to allow full coverage of the support. Additionally, the Pall membranes likely have positively charged surfaces that should support polyelectrolyte deposition.

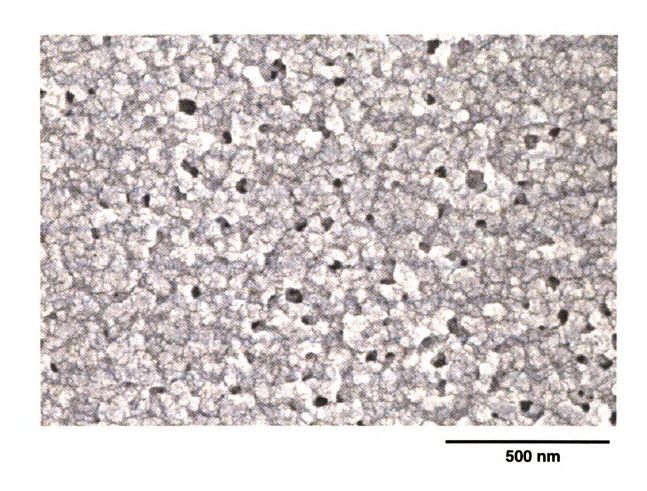


Figure 3.1: Field emission scanning eletron microscopy (FESEM) image of the surface of a bare Pall Corporation 100 kD ultrafiltration membrane. The applied potential was 10 kV. Pore sizes range from about 45 nm to 70 nm.

Unfortunately, however, although the uncoated ultrafiltration membranes allow a reasonably high water flux, deposition of 5 bilayers of PSS/PAH on these materials decreases the permeate flux to values well below those of current commercial NF membranes. Along with this decrease in flux, ion rejection is much less than that with polyelectrolyte films deposited on alumina, suggesting that either there are defects in the film or the film structure is different on the ceramic and polymeric supports. Thus, to utilize polymeric supports, we would have to either modify the support or alter the polyelectrolyte film.

To better cover the polymer support and still achieve a reasonable flux, we decided to first deposit a highly permeable, nonselective polyelectrolyte film on the support and then coat this film with a selective skin layer. This non-selective base film is often referred to as a gutter layer. Recently Tieke et al. 1,2 showed that PSS/poly(diallyldimethylammonium chloride) (PDADMAC) films on polyacrylonitrile/polyethyleneterephthalate supports provide high flux, lowselectivity membranes for pervaporation separations of ethanol and water. In water, PSS/PDADMAC films tend to swell much more than PSS/PAH films.<sup>3,4</sup> and for NF, this results in a much higher rate of water passage as well as a lower ion rejection. The use of an ultrathin, selective layer on top of the PSS/PDADMAC may result in both high flux and high ion rejections. chapter explores the use of PSS/PDADMAC films as gutter layers on both alumina and polymeric supports. The use of gutter layers on alumina results in a 33% increase in flux with little change in selectivity relative to pure PSS/PAH films. Gutter layers on polymer supports also allow formation of selective membranes, but these membranes seem to be greatly affected by the presence of divalent cations.

#### **Experimental**

#### **Materials**

Poly(diallyldimethylammonium chloride) (PDADMAC; Mw = 100,000 – 200,000; 20 wt% in water; Aldrich) (stucture shown in Figure 3.2) was used as received. All other polyelectrolytes and salts were described in Chapter 2.

#### Polyelectrolye Deposition on Porous Alumina and Polymeric Supports

To deposit PSS/PDADMAC gutter layers, a substrate was first immersed in a solution of 0.02 M PSS (molarity is calculated with respect to monomer repeat unit for all polyelectrolytes) that contained NaCl as a supporting salt. The deposition time was 3 min and was followed by a 1 min water rinse. The substrate was then immersed for 3 min in a solution of 0.02 M PDADMAC (NaCl as supporting salt) and rinsed for 1 min with water. Subsequent bilayers were deposited in the same fashion. The concentration of the supporting salt was varied to explore its effect on the gutter layer properties. All other polyelectrolyte depositions occurred as described in Chapter 2. The ultrafiltration membranes used for polymeric supports were cut into 2.2 cm-diameter circles from a sheet provided by Pall. Before polyelectrolyte deposition, I soaked the polymeric supports in water for about 30 min to wet and pre-swell them. The alumina supports were cleaned as described previously.

# Poly(diallyldimethylammonium chloride) (PDADMAC)

Figure 3.2: Shows the chemical structure of PDADMAC.

#### Ellipsometry and Nanofiltration

Ellipsometric thickness determinations for PSS/PDADMAC films were initially performed on aluminum-coated Si wafers (200 nm of Al on Si(100)). However, because of aluminum corrosion, determination of the thicknesses of films deposited from solutions containing high salt concentrations (greater than 0.5 M NaCl) had to be done on gold substrates coated with 3-mercaptopropionic acid.<sup>5</sup> Ellipsometric and nanofiltration procedures were described in Chapter 2.

#### **Results and Discussion**

#### Gutter layer on alumina

The idea behind using a gutter layer of PSS/PDADMAC is to cover the porous surface of a support with a highly permeable, continuous layer that can be easily covered with an ultrathin, selective layer. The first step was to determine an appropriate thickness for the gutter layer. Previous work in our group showed that 4 to 5 bilayers of PSS/PAH were required to completely cover an alumina support. The thickness of such films was about 20 nm as determined from SEM images. Therefore, it was assumed that the total film (gutter layer plus selective layer) should be at least this thick. To determine the thicknesses of PSS/PDADMAC films, optical ellipsometry measurements were performed on aluminum-coated Si (when using high concentrations of salt, *i.e.* 2 M, gold coated with MPA had to be used as a substrate since the aluminum corroded). Aluminum-coated substrates are most appropriate for these experiments because they contain a charged aluminum oxide coating on their surface that

**Table 3.1:** Ellipsometric thicknesses (Å) for PSS/PDADMAC films on aluminumor gold-coated substrates as a function of the number of layers and the salt concentration present during deposition.

Salt in deposition solution	2 bilayers	3 bilayers	4 bilayers	5 bilayers
0.1 M NaCl <sup>a</sup>		63±7	103±9	142±10
0.5 M NaCl <sup>a</sup>	56±1	118±1.6		324±21
2 M NaCl <sup>b</sup>	187±2	535±43°		

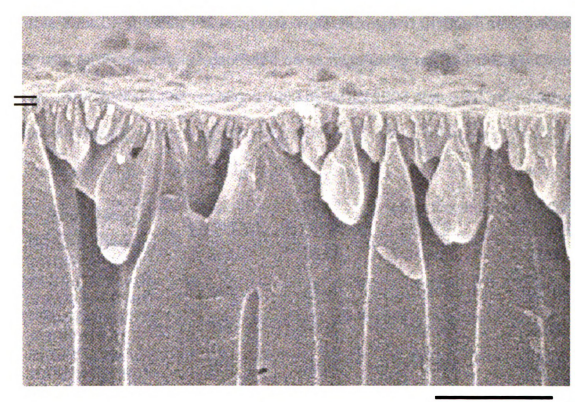
<sup>c</sup>In this case both the refractive index and thickness of the film were fit from ellipsometric data.

<sup>&</sup>lt;sup>a</sup>Film was deposited on aluminum-coated Si.

<sup>&</sup>lt;sup>b</sup>Film was deposited on gold-coated Si modified with a layer of MPA. Because this surface is negatively charged, these films contain PDADMAC/PSS bilayers rather than PSS/PDADMAC

should be representative of the alumina anodiscs. Table 3.1 presents the ellipsometric thicknesses of PSS/PDADMAC films. After applying 1.5 bilayers of PSS/PAH on top of the 3 bilayer gutter layer deposited from 0.1 M NaCl or 0.5 M NaCl, the total film thickness on porous alumina is about 300 Å as shown in Figure 3.3. This is somewhat thicker than the film on aluminum measured by ellipsometry (210 Å), however, it should be enough to coat the porous surface and allow for separation. Table 3.1 also shows that gutter layer thickness increases with NaCl concentration, as anticipated.<sup>6</sup> The use of NaCl in a deposition solution should thus allow for a full substrate coverage with fewer deposition steps.

Initial NF experiments with membranes prepared using a PSS/PDADMAC gutter layer utilized alumina as the support. This allows for comparison with the NF membranes that were prepared without a gutter layer (Chapter 2). As shown in Table 3.2, the use of 3 bilayers of PSS/PDADMAC capped with 1.5 bilayers of PSS/PAH (the final layer of PSS was deposited from 2.5 M MnCl<sub>2</sub>) yields a water flux of 2.5 m<sup>3</sup>m<sup>-2</sup>d<sup>-1</sup>, which is about 33% higher than the flux through a 4.5-bilayer PSS/PAH membrane with the final layer being deposited from 2.5 M MnCl<sub>2</sub> (see Table 2.1). Even with the increased permeate flux, the Cl<sup>-</sup>/SO<sub>4</sub><sup>2-</sup> selectivity is essentially the same for the two types of membranes. Thus, for Cl<sup>-</sup>/SO<sub>4</sub><sup>2-</sup> separations, the PSS/PDADMAC gutter layer is quite promising. Careful control over the thickness of the gutter layer is important, however, as shown by the fact that flux decreases more than two-fold when using a 5-bilayer rather than a 3-bilayer gutter layer. The salt concentration present during gutter layer deposition



500 nm

**Figure 3.3:** Cross-sectional FESEM image of [PSS/PDADMAC]<sub>3</sub>[PSS/PAH]PSS deposited on porous alumina. The applied potential for this photo was 15 kV. The final PSS layer was deposited from 2.5 M MnCl<sub>2</sub>. The thickness of the film is about 300 Å.

**Table 3.2:** Cl<sup>-</sup> and SO<sub>4</sub><sup>2-</sup> % rejections, water fluxes and Cl<sup>-</sup>/SO<sub>4</sub><sup>2-</sup> selectivities for NF with MPF membranes deposited on alumina using a PSS/PDADMAC gutter layer. The feed solution contained 1000 ppm Cl<sup>-</sup> / 1000 ppm SO<sub>4</sub><sup>2-</sup> pressurized to 4.8 bar (70 psi).

Membrane	CI <sup>-</sup> % rejection	SO <sub>4</sub> <sup>2-</sup> % rejection	water flux in m <sup>3</sup> m <sup>-2</sup> d <sup>-1</sup>	Cl <sup>-</sup> /SO <sub>4</sub> <sup>2-</sup> selectivity
[PSS/PDADMAC] <sub>2</sub> [PSS/PAH] PSS* <sup>†</sup>	2±3	94±2	3.0±0.5	17±6
[PSS/PDADMAC] <sub>3</sub> [PSS/PAH] PSS* <sup>†</sup>	3±3	97±1	2.5±0.2	32±6
[PSS/PDADMAC] <sub>5</sub> [PSS/PAH] PSS* <sup>†</sup>	5±3	97±1	1.0±0.2	38±10
[PSS/PDADMAC] <sub>3</sub> [PSS/PAH] PSS* <sup>‡</sup>	2±3	98±1	2.1±0.4	48±10
[PSS/PDADMAC] <sub>4</sub> [PSS/PAH] PSS* <sup>‡</sup>	5±3	98±0.1	2.4±0.2	43±2
[PSS/PDADMAC] <sub>3</sub> [PSS/PAH] PAA**	-1±1	96±1	1.3±0.1	28±6

<sup>\*</sup> Final layer PSS was deposited from a solution containing 2.5 M MnCl<sub>2</sub>

<sup>\*\*</sup> PAA layer deposited from 0.5 M NaCl

<sup>&</sup>lt;sup>†</sup> Gutter layer was deposited from 0.5 M NaCl

<sup>&</sup>lt;sup>‡</sup> Gutter layer was deposited from 0.1 M NaCl

should also affect flux. Changes in the ionic strength of the deposition solution affect both film thickness and film structure. A high salt concentration will yield a much thicker film that is very loopy in nature because there is a high degree of charge screening during the deposition process.<sup>7</sup> This also causes there to be a lesser degree of interpenetration between bilayers, since the charge screening reduces the charge density in each individual layer. The benefit of using higher ionic strengths during deposition would be that it would take fewer bilayers to get a defect free coating over the porous support. However, there are negative effects. Using 2 M NaCl solutions to deposit the PSS/PDADMAC gutter layer causes the water flux to decrease to 1 m<sup>3</sup>m<sup>-2</sup>d<sup>-1</sup> when only 2 bilayers of this gutter layer are deposited beneath a PSS/PAH/PSS (final PSS from 2.5 M MnCl<sub>2</sub>) capping layer. However, fluxes were similar when gutter layers were deposited using either 0.1 M or 0.5 M NaCl as a supporting electrolyte (Table 3.2). For the most part, I employed 0.1 M NaCl as it should yield thinner gutter layers.

The membrane capped with PAA yielded less encouraging results than membranes capped with PSS/PAH. In the PAA case, the flux increased only slightly over the non-gutter layer membranes discussed previously (compare Table 3.2 with Table 2.1) Additionally, the Cl<sup>-</sup>/SO<sub>4</sub><sup>2-</sup> selectivity dropped from 80 to 28. The may reflect a change in the PAA morphology that is induced by the underlying film.<sup>8</sup>

To further examine the potential utility of membranes containing a PSS/PDADMAC gutter layer, I performed NF using feed solutions containing

**Table 3.3:** Water flux and % rejection values in NF of CaCl<sub>2</sub> and MgSO<sub>4</sub> solutions by MPFs containing a PSS/PDADMAC gutter layer on alumina. The system was pressurized to 4.8 bar (70 psi).

_	1000 ppm C	a <sup>2+</sup> source	1000 ppm Mg <sup>2+</sup> source		
Membrane	water flux (m <sup>3</sup> m <sup>-2</sup> d <sup>-1</sup> )	% rejection	water flux (m <sup>3</sup> m <sup>-2</sup> d <sup>-1</sup> )	% rejection	
[PSS/PDADMAC] <sub>3</sub> [PSS/PAH] <sub>2</sub> * <sup>†</sup>	1.2±0.3	94±1	1.2±0.1	95±0.2	
[PSS/PDADMAC] <sub>3</sub> [PSS/PAH] PSS* <sup>†</sup>	1.6±0.4	79±2	1.5±0.3	93±1	

<sup>\*</sup>PSS layers were deposited from 0.5 M MnCl<sub>2</sub> solutions, and PAH was deposited from 0.5 M NaBr solutions.

<sup>&</sup>lt;sup>†</sup>Gutter layer was deposited from 0.1 M NaCl solutions.

Ca<sup>2+</sup> and Mg<sup>2+</sup>. A comparison of Table 3.3 and Table 2.1, shows that the rejection of these two cations by gutter-layer-containing membranes is within 8% of the rejection with 4.5-bilayer PSS/PAH membranes. Unfortunately, however, the permeate flux is essentially the same for the two types of membranes. Thus, the gutter layer is not serving its purpose of allowing an increased flux. This may be due to adsorption of Ca<sup>2+</sup> or Mg<sup>2+</sup> by PSS/PDADMAC and a resultant decrease in the swelling of the gutter layer.<sup>9</sup>

#### Multilayered Polyelectrolyte Films on Polymeric Supports

After analyzing the properties of alumina-supported PSS/PDADMAC films capped with PSS/PAH bilayers, I examined the possibility of using such films on a polymeric support. Because there is less charge to support film growth on a polymer surface than on alumina, development of gutter layers that can fully cover polymer supports may be especially important. In examining the potential polymer supports provided by Pall, the pure water flux of the bare supports was first measured. The poly(ethersulfone) (PES) 100 kD ultrafiltration membrane had a pure water flux of about 10 m³m⁻²d⁻¹. This is about 5 times the flux through coated alumina membranes so use of this support may be feasible. However, it should be noted that flux through the PES 100 membrane is only about 6% of that through bare porous alumina. Using a feed solution of 1000 ppm Cl⁻/ 1000 ppm SO₄²⁻, the flux decreased to about 5 m³m⁻²d⁻¹, and there was no selectivity between Cl⁻ and SO₄²⁻. The flux decline suggests that the salt solutions may

modify the membrane because there should be a minimal effect of osmotic pressure as rejections of both of the ions were less than 10%.

After investigating the properties of the bare polymer support. I began preparing MPFs on these materials. Initially a gutter layer of 5 bilayers was employed, rather than 3 bilayers of PSS/PDADMAC because I was concerned about fully covering the support. On top of the 5 bilayers, 1.5 bilayers of PSS/PAH was deposited, with the final layer of PSS being deposited from 2.5 M MnCl<sub>2</sub>. Table 3.4 shows the Cl<sup>-</sup>/SO<sub>4</sub><sup>2</sup> selectivities and flux values for these membranes in NF experiments with a feed solution containing 1000 ppm Cl<sup>-</sup> /1000 ppm SO<sub>4</sub><sup>2-</sup> (sodium salts). The permeate flux of 1.8 m<sup>3</sup>m<sup>-2</sup>d<sup>-1</sup> compares well with the 2.5 M MnCl<sub>2</sub>-terminated PSS membranes on alumina. However, the selectivity of 16 is about half of that for a similar membrane on alumina. I though that this might be due to defects in the film, so I prepared a similar membrane with a 7-bilayer gutter layer. The selectivity remained 16, but the flux decreased by 11%. Deposition of an additional PAH/PSS bilayer on the capping layer also did not achieve better selectivity, only a lower flux. Comparison of Figure 3.4 and Figure 3.1 suggests that deposition of 7-bilayers of PSS/PDADMAC and 1.5 bilayers of PSS/PAH does fully cover PES 100. The pore structure seen in Figure 3.1 is completely obscured by the polyelectrolyte film. Although there is some structure seen on the surface of the coated membrane in Figure 3.4, such patterns were previously observed with polyelectrolyte films deposited on both solid and porous substrates.<sup>3,8,10</sup> Full coverage of the support suggests that the lower selectivity of films deposited on polymer supports may be due to a modified

**Table 3.4:** Percent rejection of Cl<sup>-</sup> and SO<sub>4</sub><sup>2-</sup> as well as the water flux in NF with various membranes prepared by MPF deposition on a PES 100 support. The calculated Cl<sup>-</sup>/SO<sub>4</sub><sup>2-</sup> selectivities are also shown. The feed solution contained 1000 ppm Cl<sup>-</sup>/ 1000 ppm SO<sub>4</sub><sup>2-</sup> pressurized to 4.8 bar (70 psi).

Membrane	Cl <sup>-</sup> % rejection	SO <sub>4</sub> <sup>2-</sup> % rejection	water flux in m <sup>3</sup> m <sup>-2</sup> d <sup>-1</sup>	Cl <sup>-</sup> /SO <sub>4</sub> <sup>2-</sup> selectivity
Bare PES 100	-1±1	7±1	3.9±1.9	1±0
[PSS/PDADMAC] <sub>5</sub> †	-8±2	68±2	2.9±0.2	3±0.1
[PSS/PDADMAC] <sub>5</sub> [PSS/PAH] PSS* <sup>†</sup>	2±3	93±2	1.8±0.3	16±5
[PSS/PDADMAC] <sub>7</sub> [PSS/PAH] PSS* <sup>†</sup>	2±1	94.0±0.2	1.6±0.2	16±1
PSS/PDADMAC] <sub>5</sub> [PSS/PAH] <sub>2</sub> PSS* <sup>†</sup>	6±2	92±3	1.6±0.2	14±6
PSS/PDADMAC] <sub>7</sub> [PSS/PAH] <sub>2</sub> PSS* <sup>†</sup>	2±4	93±3	1.3±0.2	16±6
PSS/PDADMAC] <sub>5</sub> [PSS/PAH] PAA** <sup>†</sup>	-2±1	77±11	1.3±0.1	5±2
T		~ 4 . 4 . 4 . 4 . 4 . 4 . 4 . 4 . 4 . 4		

<sup>&</sup>lt;sup>f</sup>The gutter layer was deposited from a 0.1 M solution of NaCl.

<sup>\*</sup>The final PSS layer was deposited from a 2.5 M MnCl<sub>2</sub> solution.

<sup>\*\*</sup>The PAA layer was deposited from a 0.5 M NaCl solution.

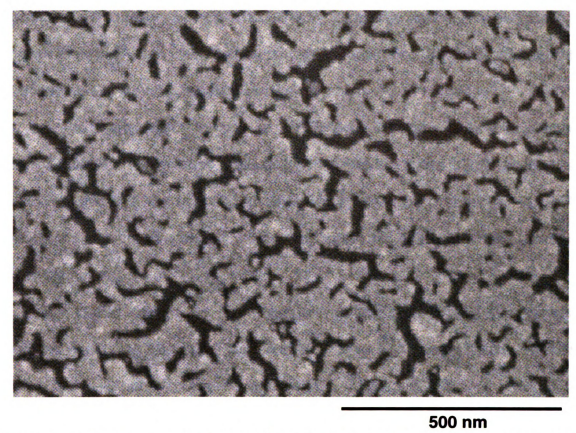


Figure 3.4: FESEM image of a [PSS/PDADMAC]<sub>7</sub>[PSS/PAH]PSS film (final PSS layer deposited from 2.5 M MnCl<sub>2</sub>) deposited on PES100. The applied potential was 10 kV.

film structure that arises from the initial support charge density and/or morphology. However, although the Cl<sup>-</sup>/SO<sub>4</sub><sup>2-</sup> selectivity on the polymer support is lower than that when using coated porous alumina, a selectivity of 16 may still be acceptable in industrial applications if flux is high.

I also attempted to use a PSS/PAH/PAA cap on 5-bilayers of PSS/PDADMAC to increase selectivity. However, these films yielded a selectivity of only 6, as opposed to selectivities of up to 80 observed for PAA hybrids on alumina (Table 2.1). This may again be due to a change in film morphology.

To further assess the NF properties of MPFs on PES 100 supports, solutions containing 1000 ppm Ca<sup>2+</sup> and 1000 ppm Mg<sup>2+</sup> were filtered. Results with these ions were somewhat disappointing. For a [PSS/PDADMAC]<sub>5</sub>[PSS/PAH]PSS film, the rejection of Ca<sup>2+</sup> dropped from 79% to 59 % on going from an alumina to a PES100 support (final layer of PSS was deposited from 0.5 M MnCl<sub>2</sub>). The Mg<sup>2+</sup> rejection fell from 93% to 58%.

Further research is needed to better understand these results, and more work must be done in order to obtain higher rejection with PES supports. If the hydrophobicity of the polymer support is hindering development of selectivity, perhaps one could UV irradiate the PES support before depositing the polyelectrolytes. Belfort et al. showed that UV modification at 254 nm increases surface hydrophilicity by breaking the sulfur-carbon bond in the main chain, creating radicals which terminate with hydroxyl groups.<sup>11</sup> They also showed that UV irradiation helps to increase the water flux of the PES by widening the pores.

The use of such a pretreatment methods may yield thin polyelectrolyte films that fully cover the support.

It may also be possible to increase the rejection of NF membranes by annealing them at a slightly elevated temperature for a short period of time. Tieke et al showed that heating polyelectrolyte membranes at 90°C for 1 hour greatly increases their selectivity in pervaporation.<sup>2</sup> This process may remove residual water, allowing more ion pairs to form and causing the film to become There is, however, a price to paid for the higher selectivity. more dense. Annealing caused the pervaporation flux of the membrane to decrease significantly. I performed one experiment using PES 100 coated with [PSS/PDADMAC]<sub>7</sub>[PSS/PAH]<sub>2</sub>. The membrane was heated overnight (18 hours) at 60°C, since heating it at higher temperatures caused the PES 100 to curl up and become deformed. NF of a 1000 ppm Mg<sup>2+</sup> solution by this membrane resulted in a Mg<sup>2+</sup> rejection of 85%. The flux, however, decreased to 0.5 m<sup>3</sup>m<sup>-2</sup>d<sup>-</sup> 1, which may be unacceptable low. It may still be possible to adjust heating temperature and annealing times to find a situation that leads to increased rejection and a reasonable flux.

#### Conclusions

This research shows that it is possible to increase the flux through MPF films deposited on alumina by depositing an ultrathin, selective layer on a highly permeable, nonselective gutter layer. Such gutter layers should help in the goal

of creating high flux NF membranes using polymeric supports. However, much more work will need to be done to make such membranes more efficient and industrially attractive.

.

#### References:

- (1) Krasemann, L.; Tieke, B. Chem. Eng. Technol. 2000, 23, 211.
- (2) Krasemann, L.; Toutianoush, A.; Tieke, B. J. Membr. Sci. 2001, 181, 221.
- (3) Dubas, S. T.; Schlenoff, J. B. Langmuir 2001, 17, 7725.
- (4) Farhat, T. R.; Schlenoff, J. B. Langmuir 2001, 17, 1184.
- (5) Harris, J. J.; Bruening, M. L. *Langmuir* **2000**, *16*, 2006.
- (6) Dubas, S. T.; Schlenoff, J. B. *Macromolecules* **1999**, *32*, 8153.
- (7) Schlenoff, J. B.; Ly, H.; Li, M. J. Am. Chem. Soc. 1998, 120, 7626.
- (8) Stair, J. L.; Harris, J. J.; Bruening, M. L. Chem. Mater. 2001, 13, 2641.
- (9) Heyde, M. E.; Peters, C. R.; Anderson, J. E. J. Colloid Interface Sci 1975, 50, 467.
- (10) Mendelsohn, J. D.; Barrett, C. J.; Chan, V. V.; Pal, A. J.; Mayes, A. M.; Rubner, M. F. *Langmuir* **2000**, *16*, 5017.
- (11) Kilduff, J. E.; Supatpong, M.; Pieracci, J. P.; Belfort, G. *Desalination* **2000**, *132*, 133.

•

#### Chapter 4

#### Fouling and Repair of NF Membranes (Future Work)

Membrane fouling is a common problem encountered when performing NF with natural feed solutions. Fouling leads to inefficient membrane processes by both decreasing the permeation rate and diminishing the rejection of ions. In order to completely understand how MPF NF membranes will perform in practical applications, one must study their fouling properties. In this chapter, I will discuss preliminary measurements of membrane fouling, as well as a possible method for regeneration of MPFs.

Chapter 1 of this thesis described the typical events that lead to a fouled membrane. Essentially all fouling events occur at the surface of the membrane and result in the formation of a cake layer (Figure 1.2). Rinsing the membrane with a cleaning solution and then placing it back into operation can reverse many types of fouling, but typically, the membrane does not completely regain its original flux.<sup>1</sup> Irreversible fouling significantly reduces the efficiency of membrane processes.

Using MPFs as NF membranes may allow for complete repair of fouled membranes. In my envisioned regeneration, the polyelectrolyte at the surface of the membrane would be removed along with the cake layer. Subsequent adsorption of a new surface layer could restore the original performance of the membrane. Recent work shows that exposure of PAH/PSS films to pH 10 buffer does result in a decrease in film thickness, presumably because of the loss of

TH. 20-5669 polyelectrolyte layers.<sup>2</sup> Additionally, Schlenoff et al. describe using high concentrations of salt to delaminate MPFs.<sup>3</sup> Such studies suggest that it may be possible, using the right combinations of pH and ionic strength, to remove the surface polyelectrolyte layer of a from the membrane, and presumably this would also remove the fouling layer as well. After removing the top layer, it should be possible to replace it with a new skin and, therefore, create a new membrane with its original flux and rejection properties. This chapter provides evidence that the top layer(s) of MPFs on gold wafers can be removed under appropriate conditions. Additionally, I briefly discuss the possible application of these data to regeneration of NF membranes.

#### **Experimental**

#### Materials

Na<sub>2</sub>CO<sub>3</sub> (CCI), NaHCO<sub>3</sub> (Mallinckrodt), 3-mercaptopropionic acid (MPA)(Aldrich), PSS, PAH, PAA (polyelectrolytes as described previously), NaCl (Spectrum), MnCl<sub>2</sub> (Acros), NaBr (Spectrum), MgSO<sub>4</sub> (Spectrum) methanesulfonic acid (Mallinckrodt), and humic acid sodium salt (Aldrich) were used as received. Buffers contained the following compositions: pH 9 buffer-0.025 M Na<sub>2</sub>CO<sub>3</sub> + 0.25 M NaHCO<sub>3</sub>; pH 10 buffer- 0.025 M Na<sub>2</sub>CO<sub>3</sub> + 0.025 M NaHCO<sub>3</sub>; pH 11 buffer- 0.25 M Na<sub>2</sub>CO<sub>3</sub> + 0.025 M NaHCO<sub>3</sub>, buffers were adjusted to the exact pH using a pH meter by adding an insignificant (less than one percent of the original mass) a percent amount of carbonate or bicarbonate

to raise or lower the pH. The gold-coated silicon wafers used were described in chapter 2.

#### Polyelectrolyte deposition and Ellipsometry

The polyelectrolyte deposition on the gold-coated silicon wafers and alumina supports was done as discussed in Chapter 2. Ellipsometric thickness measurements were also done as described in previous chapters.

#### NF measurements

NF was performed using 20 mg/L of humic acid in a 50 ppm Mg<sup>2+</sup> (from MgSO<sub>4</sub>) feed solution. NF was run until the flux value dropped to nearly 50% of original value, at which point, the membrane was considered fouled. Ion Chromatography (IC) was performed to determine SO<sub>4</sub><sup>2-</sup> and Mg<sup>2+</sup> concentrations in the NF permeate solutions. The SO<sub>4</sub><sup>2-</sup> analysis was done as previously described in chapter 2, while the Mg<sup>2+</sup> was done using a Dionex CS12A cation column, a CSRS-ULTRA suppressor, and a methanesulfonic acid eluent. The Mg<sup>2+</sup> was quantified using a 5 point calibration curve which bracketed the expected concentration of Mg<sup>2+</sup>.

#### External Reflectance FTIR

External reflectance Fourier Transform Infrared (ERFTIR) spectra were collected using a Nicolet Magna-IR 560 spectrometer and a Pike grazing angle (80° angle of incidence) attachment. Spectra were collected using 128 scans, and a UV/ozone-cleaned gold-coated wafer was used as a background.

#### Polyelectrolyte delamination by exposure to buffer

After 5-bilayers of PAH/PSS were deposited on the surface of the gold wafers, ellipsometry and FTIR measurements were performed. Then the samples were placed in the appropriate buffer for the desired time, rinsed with milli-Q water (18 M $\Omega$ /cm) for one minute, and the thickness and IR spectrum were again obtained. Subsequently, new layers of polyelectrolytes were deposited on the samples, and ellipsometry and ERFTIR were performed again.

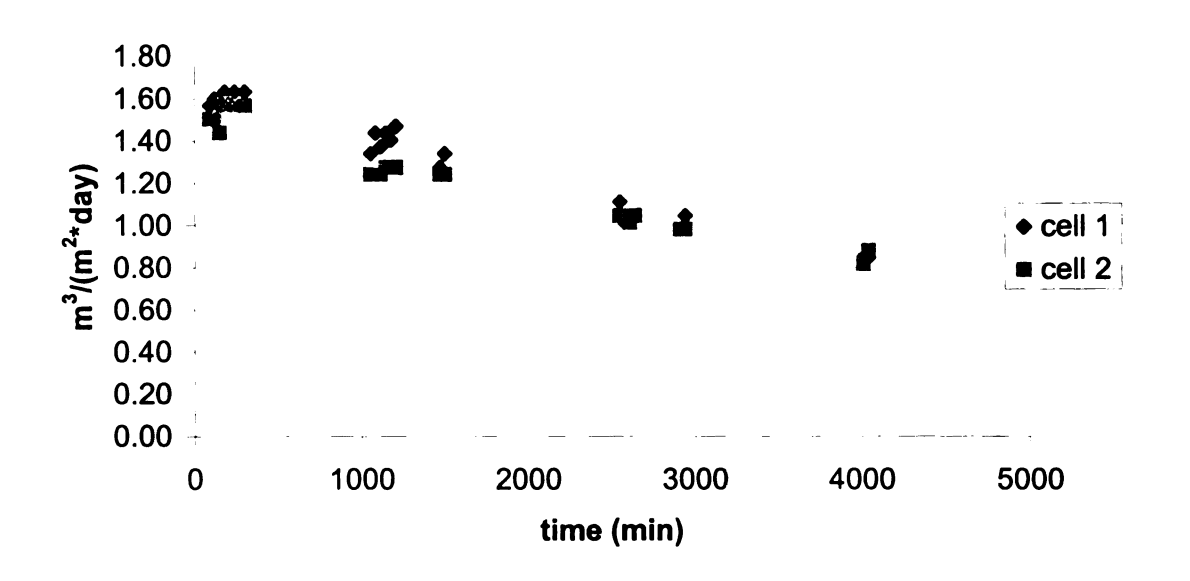
#### **Results and Discussion**

#### Preliminary data on fouling of MPF NF membranes

To gain more understanding of how MPF membranes will perform in non-laboratory settings, fouling of these materials needs to be investigated. Thus, I performed NF with a 4.5-bilayer PSS/PAH membrane on alumina using a 50 ppm Mg<sup>2+</sup> feed solution that contained 20 mg/L of humic acid. The humic acid simulates insoluble natural organic matter (NOM) found in natural water sources. Both flux and ion rejection (both Mg<sup>2+</sup> and SO<sub>4</sub><sup>2-</sup>) were measured until the water flux through the membrane was 50% of the initial flux (initial flux was measured after a 1 hr equilibration period). When the flux decreased to half the original value (68 hrs of nanofiltration), the membrane was considered fouled. The recorded water fluxes and ion rejections are plotted in Figures 4.1, 4.2, 4.3. The data show a steady decline in both flux and rejection over time. The rejection decline can be partially explained by an increase in the ion concentration in the feed solution. Over time water is leaving the system, but a high percentage of

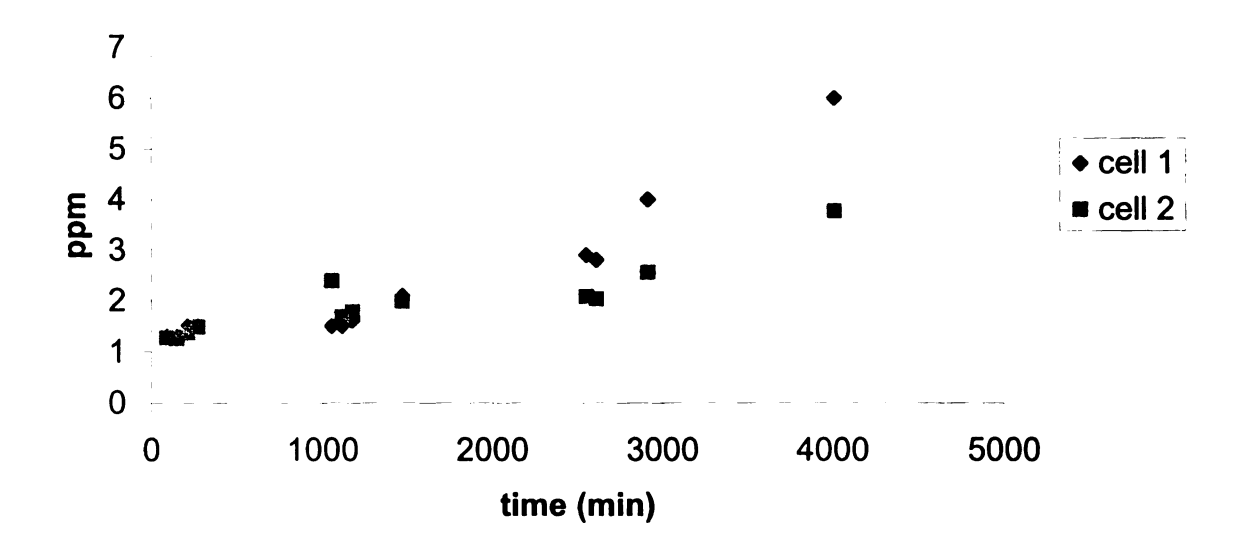
1H 20 5669

**Figure 4.1:** Plot of water flux vs. time for the NF of a 50 ppm Mg<sup>2+</sup> solution (added as MgSO<sub>4</sub>) containing 20 mg/L of humic acid. Nanofiltration was performed using a feed pressure of 4.8 bar (70 psi).



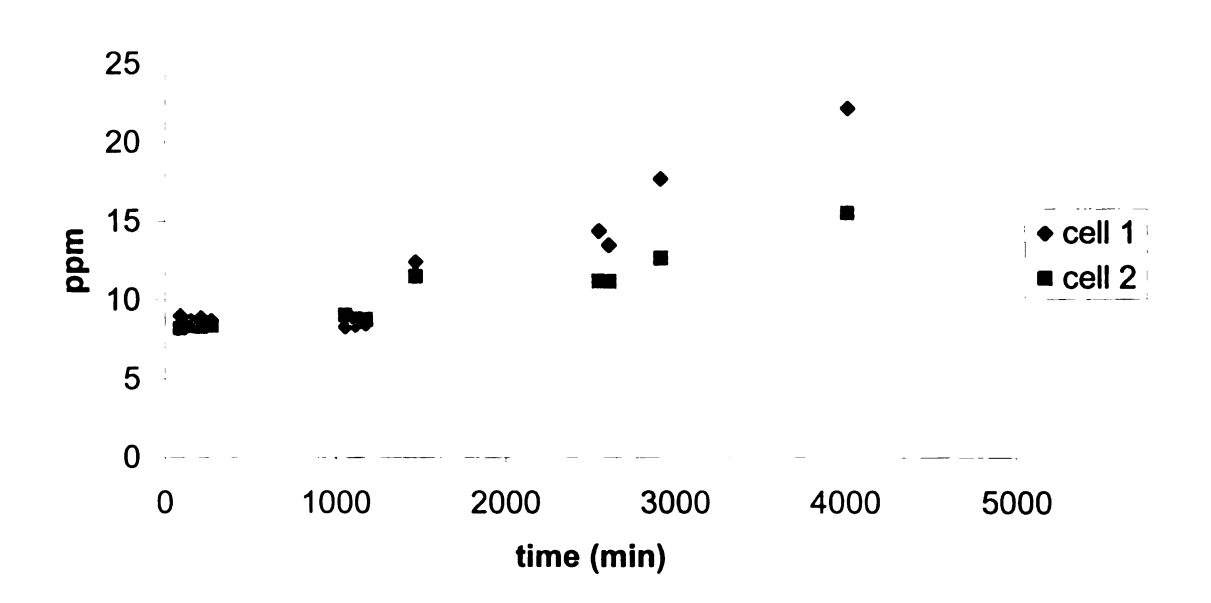
TH 20 5660

**Figure 4.2:** Plot of the Mg<sup>2+</sup> concentration in the permeate when filtering a solution of 50 ppm Mg<sup>2+</sup> with 20 mg/L humic acid. Nanofiltration was performed using a feed pressure of 4.8 bar (70 psi).



TH, 20, 5662

**Figure 4.3:** Plot of SO<sub>4</sub><sup>2-</sup> concentration in the permeate solution vs. time when filtering a 50 ppm Mg<sup>2+</sup> (from MgSO<sub>4</sub>) solution containing 20 mg/L of humic acid. Nanofiltration was performed using a feed pressure of 4.8 bar (70 psi).



1H  the ions are being rejected. These leads to a 34% increase in the feed concentration over the 68 h period. However, this does not account for all the ion rejection decline because the permeate Mg<sup>2+</sup> concentration increased by 200 to 350%. Thus, the fouling layer must be mostly responsible for the rejection change. This change in rejection may be from a decrease in the charge from the PSS caused by the adsorbed material on the surface. In the future, this assessment of the membranes will need to be carried out with other potential fouling agents such as silica particles or bacteria.

Vrijenhoek et al. demonstrated that the rate of membrane fouling is often related to surface roughness of the membrane.<sup>4</sup> Thus, AFM measurements of the rougheness of MPFs on alumina also need to be performed. This will allow comparison of the fouling data with that for other NF or ultrafiltration membranes.

## Repairing Fouled MPF membranes

As discussed earlier, fouling occurs primarily at the membrane surface. To clean and repair a fouled MPF NF membrane, it may be possible to remove the surface layer and replace it with a new layer. To investigate this concept, 5-bilayer PAH/PSS films on gold surfaces were placed in high pH buffers for various time periods. The high pH should cause deprotonation of PAH, and hence loss of its positive charge. Once this occurs, the electrostatic interactions between PAH and PSS will decrease so that the PAH can be rinsed away, as long as there is minimal interpenetration between the PAH and PSS.

TH 20 5663

Table 4.1 and Figure 4.4 show the results of experiments aimed at delaminating films using high pH solutions. Table 4.1 demonstrates that films do become thinner after exposure to the buffers, presumably due to delamination. However, the amount of thickness lost does not necessarily increase with buffer pH. The pH 9 buffer removed a greater thickness of the film than the pH 10 buffer. One reason for this may be the greater ionic strength of the pH 9 buffer. Both buffers were made from Na<sub>2</sub>CO<sub>3</sub> and NaHCO<sub>3</sub> using 0.025 M Na<sub>2</sub>CO<sub>3</sub>. However, to achieve the appropriate pH value, the pH 9 buffer contained 0.25 M NaHCO<sub>3</sub>, 10-fold more than the amount in the pH 10 buffer.

The higher salt concentration in the pH 9 buffer may cause a polyelectrolyte film to come apart by increasing the osmotic pressure<sup>3</sup>. An experiment performed using a pH 10 buffer with ten times the carbonate and bicarbonate concentrations showed about 70% removal of the film in 5 min, thus confirming the ionic strength effect. I also added 0.25 M NaCl to the original pH 10 buffer. This resulted in a loss of 20% of the original film thickness during a 5 min immersion time. The pH 10 buffer with 0.25 M NaCl yields nearly identical results in 5 min as those seen for the pH 9 buffer in 10 min of immersion time.

Since the goal in repairing a fouled membrane is the removal and replacement of only the surface layer (or bilayer), conditions that result in loss of about 20% of the thickness of a 5-bilayer film are desirable. The results in Table 4.1 show that submersion in pH 9 buffer for 10 minutes gives the desired removal. Furthermore, re-depositing the PAH/PSS layer restores the original thickness, and therefore, may yield a rejuvenated membrane with its original

Table 4.1: Ellipsometric thickness values (Å) for 5-bilayer PAH/PSS films before and after submersion in buffer solutions for the indicated time, and after a PAH/PSS layer was re-deposited to see if the original thickness could be obtained.

Buffer pH	Immersion time (min)	Thickness before buffer	Thickness After exposure to buffer and rinsing	% of film removed by the buffer	Thickness after redeposition of a PAH/PSS layer
9 <sup>a</sup>	2	198±8	179±16	10±6	219±7
9 <sup>a</sup>	5	193±9	161±10	17±4	211±25
9 <sup>a</sup>	10	195±13	159±10	18±2	195±13
9 <sup>a</sup>	20	201±2	156±7	23±2	189±3
9 <sup>a</sup>	30	197±11	142±8	28±7	185±3
10 <sup>b</sup>	2	190±8	184±7	3±3	226±4
10 <sup>b</sup>	5	189±11	177±10	6±1	215±17
10 <sup>b</sup>	10	195±4	181±6	7±4	223±2
10 <sup>b</sup>	20	193±6	178±8	8±3	216±5
10 <sup>b</sup>	30	194±12	177±9	9±3	216±8
11 <sup>c</sup>	2	197±4	139±13	29±6	182±19
11 <sup>c</sup>	5	195±13	134±7	31±2	170±12
11 <sup>c</sup>	10	200±4	130±3	35±2	167±4
11 <sup>c</sup>	20	194±15	121±5	38±3	168±6
11 <sup>c</sup>	30	205±15	128±7	38±1	176±7

<sup>&</sup>lt;sup>a</sup> pH 9 buffer contained 0.025 M Na<sub>2</sub>CO<sub>3</sub> + 0.25 M NaHCO<sub>3</sub>

<sup>&</sup>lt;sup>b</sup> pH 10 buffer contained 0.025 M Na<sub>2</sub>CO<sub>3</sub> + 0.025 M NaHCO<sub>3</sub>

<sup>&</sup>lt;sup>c</sup> pH 11 buffer contained 0.25 M Na<sub>2</sub>CO<sub>3</sub> + 0.025 M NaHCO<sub>3</sub>

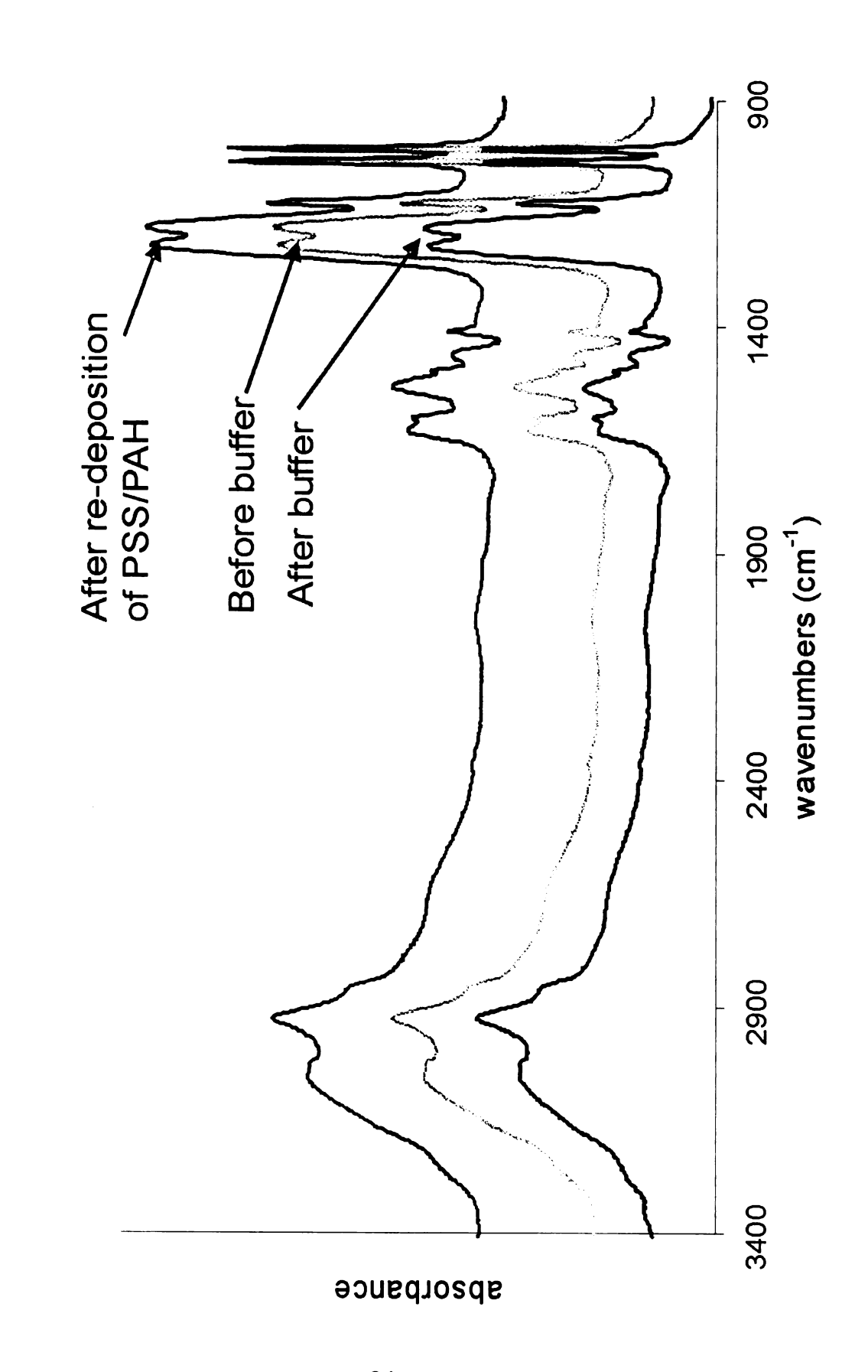
properties.

FTIR spectra (Figure 4.4) also show that absorbance bands return to their original levels after immersion of a film in pH 9 buffer and adsorption of a new PAH/PSS bilayer. (See table 4.2 for peak intensities) This provides further evidence for the removal and replacement of the surface layer.

Submerging the sample in a pH 9 buffer solution for longer times (20 to 30 min), probably starts removal of a second layer. In this case, the re-deposition step yields a film that is thinner than the original. Using pH 11 buffer appears to remove two bilayers almost immediately, as shown by the ellipsometric thickness and FTIR measurements. This buffer may be too harsh for the goal of removing the surface. Further research also needs to be done on films capped with PAA. Immersion in pH 9 buffer for 2 min resulted in the removal of one bilayer from a PAA-capped film. Longer periods of time resulted in at least 2 bilayers being removed from the surface. The time has to be monitored carefully in this case, since the PAA layer appears to be removed very quickly in high pH buffer. This likely allows the buffer solution to permeate the film more quickly and remove more layers.

The next step in this research will be to remove the surface layer from a membrane in the NF setup. The experiment that is planned for this case involves flowing a buffer solution across the membrane in the cell for a set amount of time, followed by a rinse and subsequent re-deposition steps. The difficult part will be determining the amount of time to flow the buffer across the membrane to obtain the desired results. This will be especially challenging

Figure 4.4: ERFTIR spectrum of PAH/PSS films on a gold-coated silicon wafer



TH

Table 4.2: Absorbances (abs) for 3 main peaks in the spectra in Figure 4.4.

Peak	Abs before buffer	Abs after buffer	Abs after re- deposition
1180 cm <sup>-1</sup>	0.0117	0.0085	0.0116
1220 cm <sup>-1</sup>	0.0116	0.0083	0.0115
2920 cm <sup>-1</sup>	0.0069	0.006	0.0072

because of the difficulty of characterizing membranes on porous supports. I attempted to use Brewster angle FTIR to examine layer removal from alumina, but the alumina support absorbs below the 1250 cm<sup>-1</sup> region, masking the strongest bands (sulfonates) of PSS/PAH films. Therefore, the timing of the removal and re-deposition steps may have to be done empirically by measuring flux and rejection both before fouling and after re-deposition.

## Conclusion

Preliminary measurements show that MPF membranes foul significantly in the presence of humic acids. However, MPF NF membranes may offer a very effective method for membrane regeneration. Experiments with films on gold-coated wafers show that it is possible to remove the surface layer of the MPF using high pH buffer solutions. The removed layers can be replaced by re-immersing the wafers in the PAH and PSS deposition solutions. Future research will involve regeneration of fouled membranes in NF cells.

## References:

- (1) Kilduff, J. E.; Mattaraj, S.; Sensibaugh, J.; Pieracci, J. P.; Yuan, Y.; Belfort, G. *Environmental Engineering Science* **2002**, *19*, 477.
- (2) Harris, J. J.; Bruening, M. L. *Langmuir* **2000**, *16*, 2006.
- (3) Dubas, S. T.; Schlenoff, J. B. *Macromolecules* **2001**, *34*, **3736**.
- (4) Vrijenhoek, E. M.; Hong, S.; Elimelech, M. J. Membr. Sci. 2001, 188, 115.

